



UNIVERSITÀ
DEGLI STUDI
DI PADOVA

Università degli Studi di Padova

Dipartimento di Ingegneria Industriale
Corso di Magistrale in Ingegneria Elettrica

Tesi di Laurea Magistrale

**Electrodynamic transients in the ITER electrical
network due to MV motor starting and faults on
the supply grid**

Relatore: Prof. Roberto TURRI

Correlatori: Ivone BENFATTO, David BALAGUER (ITER Organization)

Laureando: Davide CORDIOLI

Anno Accademico 2014/2015

Summary

Introduction

1. ITER Plant	3
1.1 Overview.....	3
1.2 ITER Electrical Power Network.....	8
1.2.1 Pulsed Power Electrical Network.....	10
1.2.2 Steady State Electrical Network.....	11
1.2.3 Reactive Power Compensation and Harmonic Filtering.....	12
1.2.4 Coil Power Supply.....	13
1.3 Cryogenic System.....	14
2. User Guide for ETAP and SimPowerSys	17
2.1 General Information.....	17
2.2 ETAP.....	17
2.3 Matlab Simulink – SimPowerSys.....	18
2.4 Input Data for Electrical Motors.....	18
2.4.1 ETAP Specifications.....	18
2.4.2 SimPowerSys Specifications.....	20
2.5 Input Data for Transformers.....	22
2.5.1 ETAP Specifications.....	22
2.5.2 SimPowerSys Specifications.....	23
3. Input Data	27
3.1 MV Busbars JB-3000 and JB-4000.....	27
3.2 LN2 GAN Motors Data.....	28
3.2.1 Main Data.....	29
3.2.2 Electrical Model.....	29

3.2.3	Load Model.....	29
3.3	LN2 and LHe Motors Data.....	30
3.3.1	Main Data.....	31
3.3.2	Electrical Model.....	31
3.3.3	Load Connected.....	31
4.	Motor Starting Analysis.....	33
4.1	Starting Methods for Induction Motors.....	33
4.1.1	Soft Starter.....	34
4.2	Motor Starting Study.....	36
4.2.1	Criteria to Respect.....	37
4.2.2	Starting Scenarios.....	38
4.3	Analysis and Results with ETAP.....	40
4.3.1	Normal Study Case.....	42
4.3.2	Intermediate Study Case.....	43
4.3.3	Unfavourable Study Case.....	44
4.3.4	Most Unfavourable Study Case.....	45
4.4	Analysis with SimPowerSys.....	46
4.4.1	LN2 GAN Motor in SimPowerSys.....	47
4.4.2	Soft Starter in SimPowerSys.....	49
4.5	Comparison and Results.....	51
4.5.1	Differences with DOL Technique.....	52
4.5.2	Differences using the Soft Starter.....	54
5.	Voltage Reduction due to External Faults and Effects on the MV-01 Motors.....	57
5.1	Faults and Consequences on the MV Motors.....	57
5.2	External Electrical Grid.....	58
5.2.1	Known Data and Assumptions.....	60
5.3	External Grid Equivalent Model with SimPowerSys.....	62

5.4 Simulations and Results.....	65
5.5 Effects on the MV Motors.....	67
5.5.1 Voltage Source.....	70
5.5.2 Results.....	71
6. Conclusions and Future Developments.....	75
7. References.....	77

Introduction

The increasing and continuous technologic development of the last century had, and still has, a direct consequence on the growth of the worldwide energy need. In recent years several renewable energy plants have been included in the electrical grid in order to add power to that produced by the traditional plants such as the oil, coal, natural gas and fission nuclear power stations.

Even with the actual big use of renewable energy, there is a common opinion that a different and valid alternative must be provide and for several reasons: first of all the fossil fuels are not a renewable source of energy and moreover they are one of the biggest causes for pollution in the world; on the other hand, even if the energy produced with fission reaction is millions time higher than the one obtained with the process of combustion, products of discard are strongly radioactive and they require thousands of years for the disposal of the waste to reach an acceptable security level; the renewable energy are useful to reduce the problems expressed but unfortunately, due to their lack of programmability and the demand of the electric grids (for matter such as the stability), they cannot replace completely the traditional power plants.

An alternative energy source is nuclear fusion: this gives the possibility to generate an enormous quantity of power, in fact the energy gain factor (Q) is equal to 10 and so much higher than the factor of a coal fired power station ($1/3$), but also this power is “clean” and “pure” since the radioactive products have a half-life of 12.3 years. Indeed, the future fusion power plants have good prospects to be an economic benign base for electricity generation stations. The progress of fusion development has been remarkable, all available techno-scientific information shows that a significant process was made towards a successful reactor, but a lot of study and research remains to be done in order to reach the final product.

At the moment the largest project for a thermonuclear experimental reactor is ITER, the international project funded and run by seven member entities, European Union, India, Japan, China, Russia, South Korea and United States: its main goal is to make the transition from experimental studies of plasma physics to a full scale electricity fusion power plant. Within ITER project there are numerous of divisions and sections, each one specialized in a specific area of research since this is a large project.

This thesis describes the work I have done at the ITER Electrical Engineering Department: the aim of this work is to analyze the possible electrical disturbances between the Cryogenic system and the ITER electrical network, more precisely the problems that occur due to the effects of voltage drops and faults both inside and outside the ITER grid.

A part of the thesis is dedicated to the problem of the voltage drops linked to the starting process of the largest motor of the network, a 4.7 MW asynchronous motor connected to a 6.6 kV busbar: the analysis has been made considering the use of a the soft starter in order to verify some criteria and reduce the impact on the voltage.

Subsequently there are described studies regarding the effects generated by internal and external faults on the ITER Network and some of its loads, because the voltage reductions that they could bring are dangerous for the plant operation and it is important to consider the impact they could have on the load side in order to prevent problems to the entire system.

1. ITER Plant

In this chapter will be briefly summarized some basic concept regarding nuclear fusion, giving also a look at ITER Organization, specifically to the Power Supply and Cryogenic Systems.

1.1 Overview

ITER is a large scale scientific experiment to demonstrate that it is possible to realize an environmentally friendly energy source for humanity from nuclear fusion [1]. It is presently under construction in Saint Paul Les Durance in southern France and it is a unique international scientific collaboration, probably the largest undertaken by humankind.

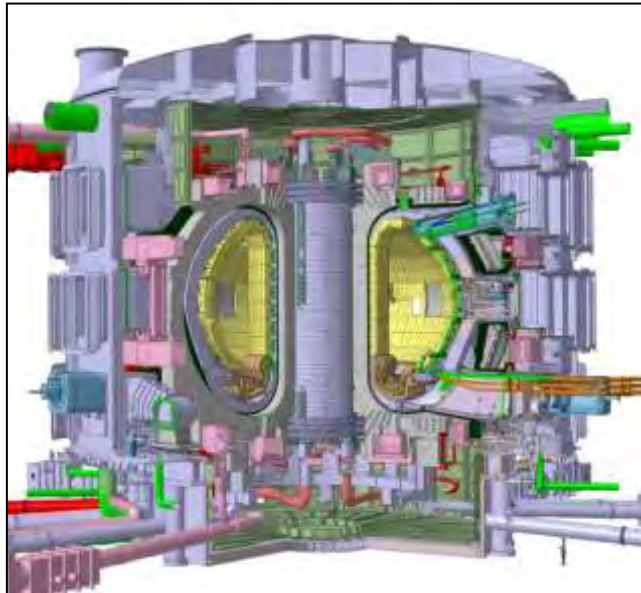


Fig. 1.1 ITER Tokamak Machine

The ITER Agreement, signed in 2006, includes the following members: People's Republic of China, the European Union, the Republic of India, Japan, the Republic of Korea, the Russian Federation and the United States of America, together representing over half of the world's population.

Fusion is the most natural phenomenon in the universe: nuclear fusion powers the Sun and the stars. In a fusion reaction, two light atomic nuclei combine form a heavier nucleus and release energy. Magnetic fusion aims at reproducing a similar reaction on Earth.

Nuclear fusion is a reaction in which light nuclei are fused to form more massive nuclei with a simultaneous release of energy as shown in Fig. 1.2.

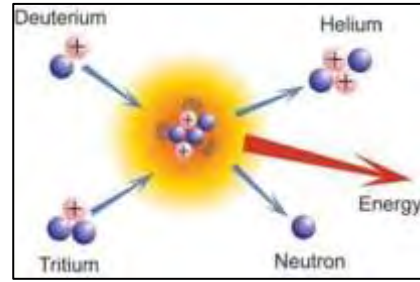


Fig. 1.2 The Fusion Reaction

From a physical point of view fusion of Deuterium and Tritium nuclei generates one neutron and 14.1 MeV Energy plus Helium 4 and 3.5 MeV Energy. To get the above nuclear reaction, fusion on the earth is simulated through the following steps [2]:

- Heat Deuterium plus Tritium (DT) plasma to more than 100 million °C;
- Keep hot plasma away from walls by strong magnetic fields (both poloidal and toroidal);
- Neutrons transfer their energy to the Blanket which works also fuel breeding;
- In a fusion power plant, conventional steam generator, turbine and alternator will transform the heat into electricity (as per Fig. 1.3). It is important to outline that 1 gram of fusion fuel is equivalent to 8 tonnes of oil.

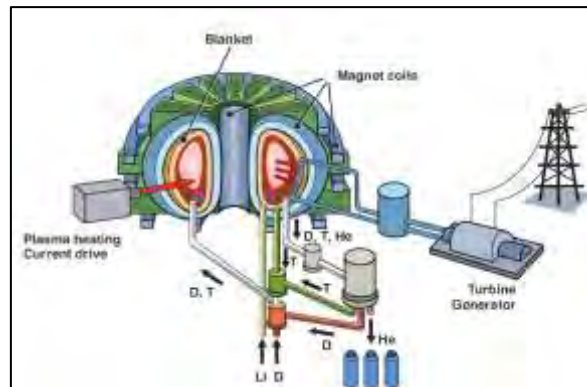


Fig. 1.3 Fusion Plant for generating energy

The overall programmatic objective of the ITER project is to demonstrate the scientific and technological feasibility of fusion energy for peaceful purposes. Its principal goal is to design, construct and operate a Tokamak experiment at a scale which satisfies this objective. ITER is designed to confine a Deuterium-Tritium plasma in which α -particle heating dominates all other forms of plasma heating: it means that ITER is a burning plasma experiment. As ultimate goal ITER will develop steady state fusion power production and will integrate and test all essential fusion power reactor technologies and components. ITER has to demonstrate safety and environmental acceptability of fusion (Fig. 1.4). The self-sustained D-T burning plasma in ITER generates 10 times more power than it receives: the input power is equal to 50 MW, the output power will be in terms of

design performance approximately equal to 500 MW: it means ITER is a power amplifier [3] [4]. For all these reasons ITER is a necessary step on the way to commercial fusion reactor.

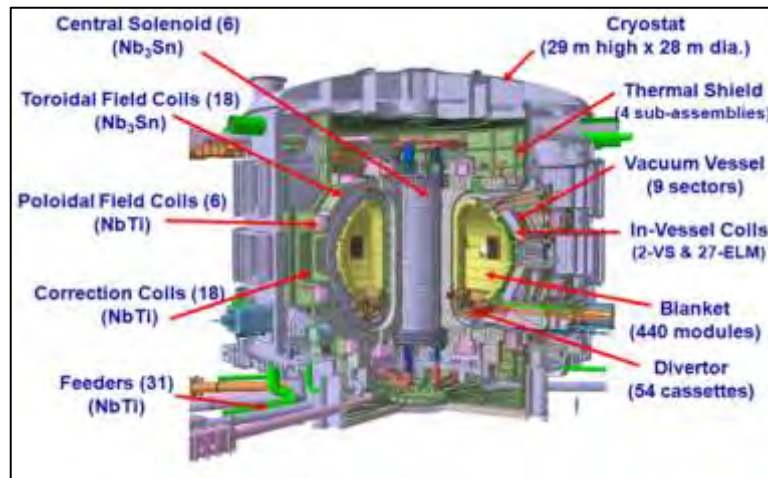


Fig. 1.4 ITER Machine Assembly – Components Identification

ITER will exploit the process by magnetic confinement of plasma whereby it is contained within toroidal vessel walls by strong magnetic fields, produced by superconducting coils surrounding the vessel and an electrical current driven in the plasma, a magnetic configuration called Tokamak.

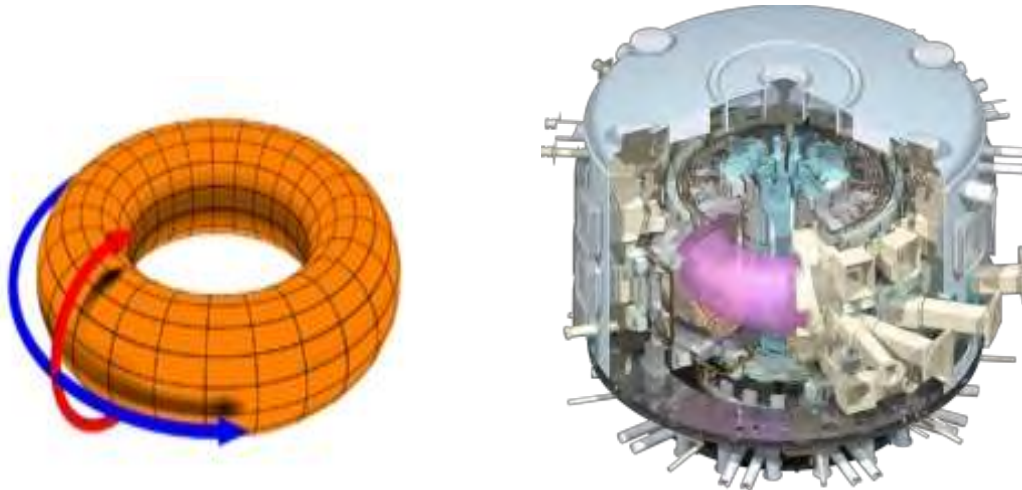


Fig. 1.5 Toroidal and Poloidal Fields in ITER Machine

The ITER Tokamak uses magnetic fields to confine plasma in the shape of a torus (donut). Stable plasma equilibrium requires magnetic field lines that move around the torus in a helical shape. The helical field is the result of adding a toroidal field (travelling around the torus in circles) and a poloidal field (travelling in circles orthogonal to the toroidal field) as per Figure 1.5.

In ITER 18 superconducting electromagnet coils surrounding the torus will produce the Toroidal Field (TF); the Poloidal Field (PF) is the result of a Toroidal electric current flowing in the plasma induced by six superconducting electromagnet coils in the Central Solenoid (CS) as per Fig. 1.6 and Fig. 1.7.

In addition, six superconducting electromagnet coils are positioned externally to permit variations of radial and vertical fields to control the plasma position and shape and there are three sets of three correction coils for stray error field compensation.

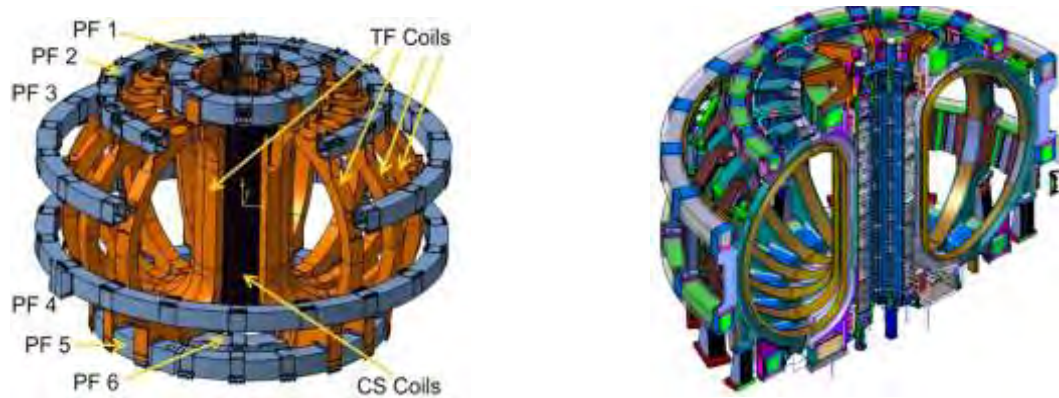


Fig. 1.6 Arrangement of Magnet Coils

Further in-vessel coils are proposed for vertical plasma stabilisation and edge phenomena or Edge Localised Modes (ELM) control.

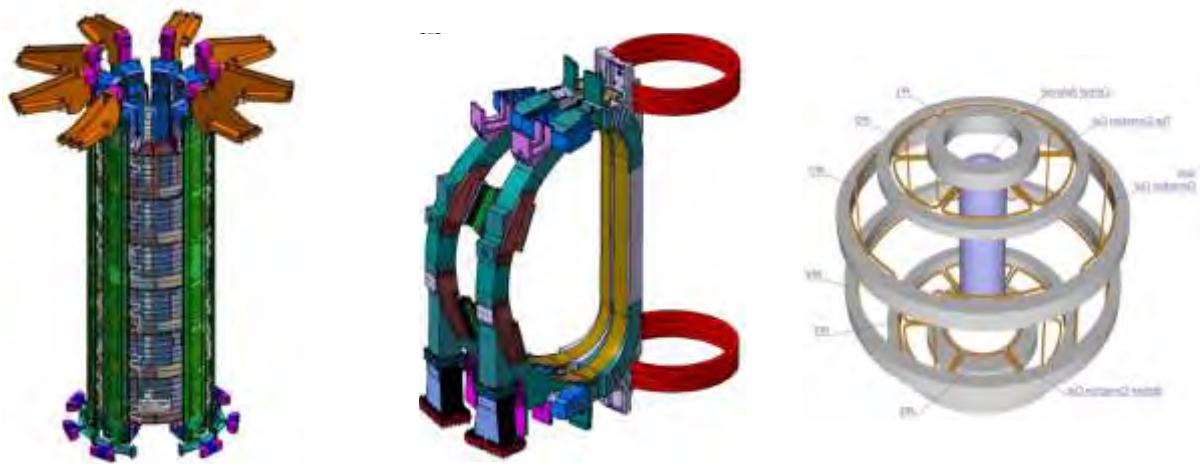


Fig. 1.7 Central Solenoid – Pair of Toroidal Field Coils – Poloidal Field Coils

Plasma has to be intended as the fourth status of the matter characterized by high energy density being a warm dense matter. Non Linear phenomena and far equilibrium state characterize Plasma behaviour.

The plasma comprises charged particles - positive nuclei and negative electrons that can be confined and shaped by magnetic fields, particles in the plasma will follow magnetic field lines.

The walls of the vacuum vessel (Fig. 1.8), the first safety confinement barrier, will not be in contact with the plasma due to the magnetic confinement with it.

Separation of the plasma and the 'first wall' vessel wall is vital to limit heat loading, damage and plasma contamination [5] [6].

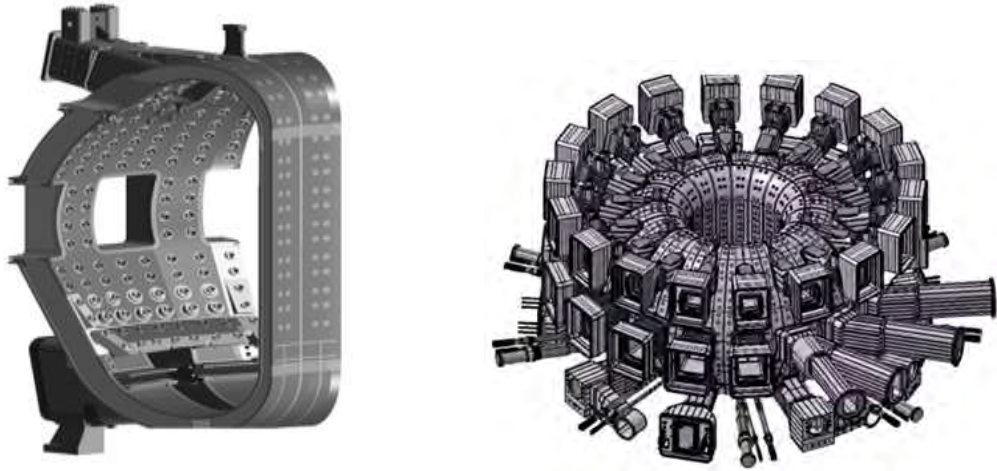


Fig. 1.8 Vacuum Vessel

All the Machine Assembly is confined into the Vacuum Barrier (named Cryostat) which has the containment function for the ITER Machine Assembly (Fig.1.9) [7].

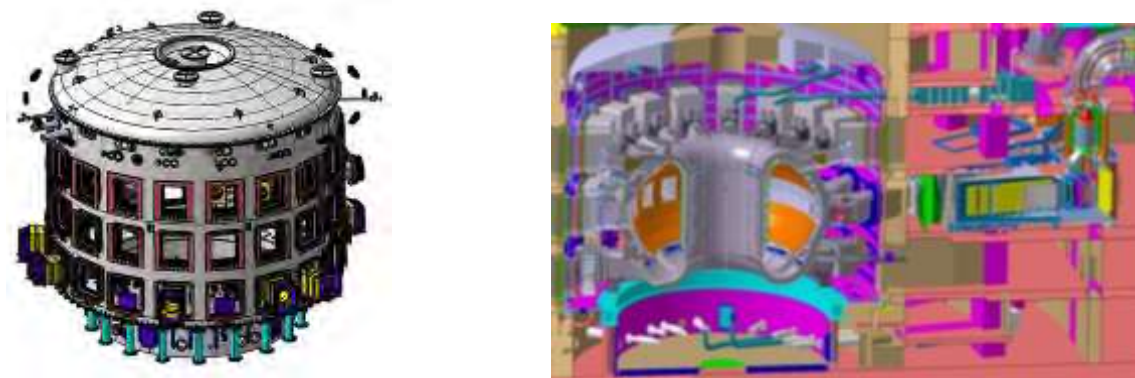


Fig. 1.9 Cryostat and vacuum system

Few questions have to be satisfied before closing the short overview in ITER project:

- How safe is ITER Machine [2] [4];
- Radioactivity Release and Radiological wastes for next generations [7] [8] [9].

Nuclear Accidents like Fukushima or Chernobyl or Three Miles Island, which represent the milestones in the Fission Reactors Story, are physically and technologically impossible because there is no reactivity factor that can diverge as for nuclear fission plants. The fusion reaction is intrinsically safe. Additionally fuel inventory is very small: less than one gram of fuel is reacting at any given moment in the reactor core. Any disturbance will

stop the plasma and the nuclear fusion reaction switches off. As a consequence runaway reactions and core-meltdown are impossible. Cooling is not a safety function: if power is lost, heat evacuation happens naturally.

In the frame of the control of radiological wastes it has to be understood that ITER will not generate long-life/high activity waste.

During normal operation, ITER's radiological impact on the most exposed populations will be one thousand times less than natural background radiation [10]. "Worst-case scenarios", such as fire in the Tritium Plant, would have a lesser impact on neighbouring populations than natural background radiation. The ITER facility is being licensed in France as a Basic Nuclear Installation (INB) and will observe French safety and security regulations. Nevertheless, as per all the other fission Nuclear reactors following Fukushima event, a stress test in the frame of WENRA and IAEA framework requirements, will be conducted by Nuclear Safety Authority to demonstrate safety margins of the ITER Machine considering beyond design basis events (Fig. 1.10).

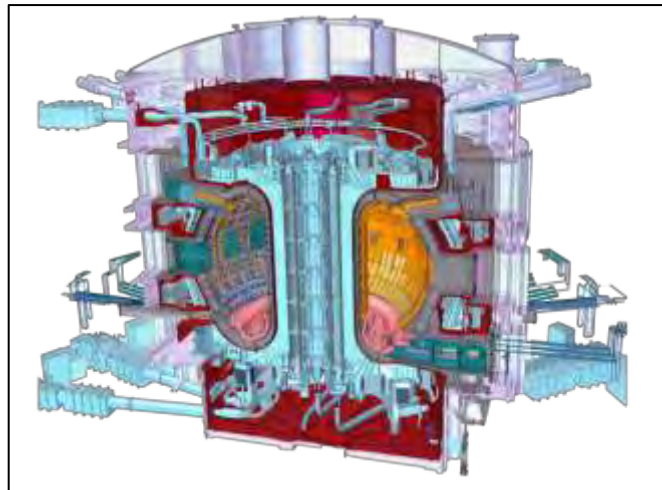


Fig. 1.10 ITER Machine Assembly and Plant

1.2 ITER Electrical Power Network

The Department for ITER Project (DIP) regroups the six technical directorates, responsible for the construction of the ITER device. The Department's goal is the timely construction of ITER. The DIP is composed of six technical directorates:

- *Tokamak (TKM)* takes care of the studies and research of the magnets (toroidal and poloidal fields, central solenoid) and the vacuum vessel;
- *Plasma Operation (POP)* deals with confinement, stability and control of plasma;
- *CODAC Heating and Diagnostic (CHD)* deals with the control system responsible for operating the ITER device, heating process and all the measurements necessary to control, evaluate and optimize plasma performance;

- *Building and Site Infrastructure* (BSI) has to ensure that the site infrastructure and buildings required are designed and constructed in a timely and cost efficient manner and in accordance with specified requirements;
- *Plant System Engineering* (PSE) is responsible for the procurement arrangements, fabrication and testing of the following systems: cooling water system, cryogenics, hot cell, fuelling and wall conditioning, tritium, maintenance and remote handling and the steady state and pulsed electrical power supply;
- *Project Control and Assembly* (PCA) is responsible for monitoring the ITER project schedule and schedule recovery actions.

The ITER Electrical Power Supplies has the aim to provide the electrical power for the ITER plant and the facilities, both in steady state and peak periods during plasma operation. Typically the power is between 130 MW and 630 MW.

ITER Network is comprehensive of the following two major systems [11] [12] [13]:

- *Pulsed Power Electrical Network* (PPEN), designed to supply AC power to the coil and also to the Heating and Current Drive (H&CD) PS. It will absorb 500 MW and 200 MVar;
- *Steady State Electrical Network* (SSEN), dedicated to provide AC power to various loads, primarily motors, within the plant systems such as cooling water system, cryoplant, buildings and HVAC as well as Tritium Plant. It will receive up to 130 MW.

There are also other two “minor” systems:

- *Reactive Power Compensation and Harmonic Filtering* (RPC&HF), used to reduce the reactive power and the voltage distortion of the grid but also the disturbances generated by the ITER plant (~ 750 MVar, the largest in Europe, most likely the 3rd largest in the world);
- *Coil Power Supplies* (CPS), useful to provide controlled DC current to the Toroidal Field and Poloidal Field coils.

Electrical power requirements for the ITER plant and facilities will range from 130 MW for steady state auxiliary supplies, plus 500 MW for peak periods (pulsed) during plasma operation. Both the PPEN and SSEN systems will be connected to the French 400 kV transmission network operated by RTE (*Gestionnaire du Réseau de Transport d'Electricité*): it is capable of providing the steady-state power required by the SSEN in addition to 500 MW, 200 MVar pulsed power for the pre-programmed PF scenarios, the plasma current, position and shape control, including vertical stabilization, the H&CD PS, the superconducting magnet coils and in the vessel coils [14]. This substation will be connected to the 400 kV grid by a double circuit line as showed in Fig. 1.11. For this aim, the current nearby 400 kV overhead line will be diverted and a new 5 km overhead line will be pulled.



Fig. 1.11 400kV and 225kV grids in the ITER area

During ITER operation, the 400 kV grid might be disturbed because of the pulsed loads. In order to evaluate and mitigate disturbances in the grid, RTE carried out a dynamic study necessary to check that these disturbances generated by ITER pulsed loads remain within an acceptable range in terms of voltage drops (maximum 3%), and concerning electromechanical constraints on power generation units.

1.2.1 Pulsed Power Electrical Network

The PPEN will supply alternating current power to the superconducting magnet coils, in-vessel coils and the Heating and Current Drives [11] [15] [16]. It will absorb 500 MW and 200 MVar pulsed power for the pre-programmed physics scenarios and plasma current, position and shape control. For the PPEN the 400 kV supply is transformed via three step-down transformers, each rated at 300 MVA continuous power to intermediate voltage (IV) at 66 kV (secondary winding - star connected) and to medium voltage (MV) at 22 kV (tertiary winding - delta connected).

The grid voltage is transformed at 66 kV and 22 kV voltage levels as required by the systems to be supplied. Most of the loads - AC/DC converters for the magnet coils of the Toroidal Field (TF), Central Solenoid (CS), Poloidal Field (PF) and Correction Coils (CC), and the H&CD PS - will be shared among the three 66 kV busbars. The loads with relatively lower power per unit, i.e. less than 20 MVA, will be connected to the 22 kV MV busbars. A simplified one-line diagram of the PPEN with the loads connected is shown in Fig. 1.12.

The power is distributed from three main 66 kV busbars and three main 22 kV busbars that will normally operate uncoupled from each other. The loads connected to PPEN are mainly large thyristors based AC/DC converters rated typically in the range from 5 to 90 MVA [18]. Most of the large and dynamic loads are directly fed from the 66 kV busbars, i.e. the AC/DC converters feeding the superconducting magnet coils and the Neutral Beam system to provide plasma current. The Loads with relatively lower power (normally less than 20 MVA/unit) are fed from the 22 kV busbars.

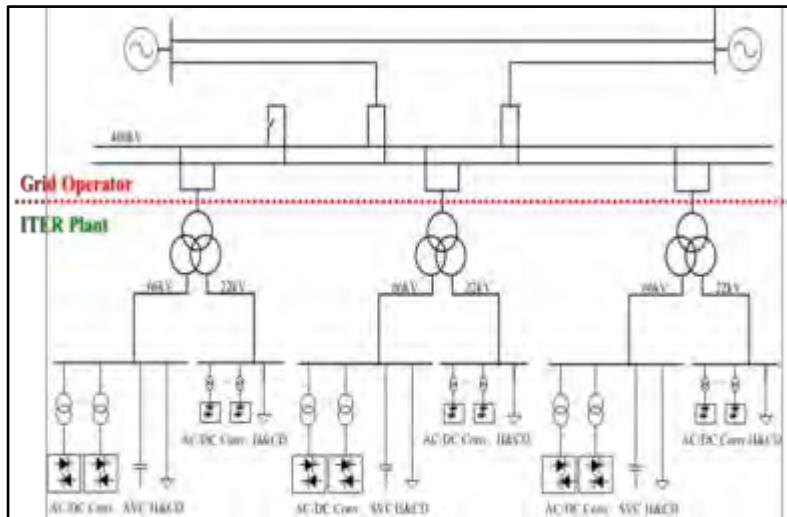


Fig. 1.12 PPEN simplified one-line diagram

Accordingly PPEN has been designed to be expanded in future in order to operate upgraded plasma scenarios demanding mainly more heating and current drive systems (extended phase). The expected total PPEN power profile at 400kV in normal operation is shown in Figure 1.13.

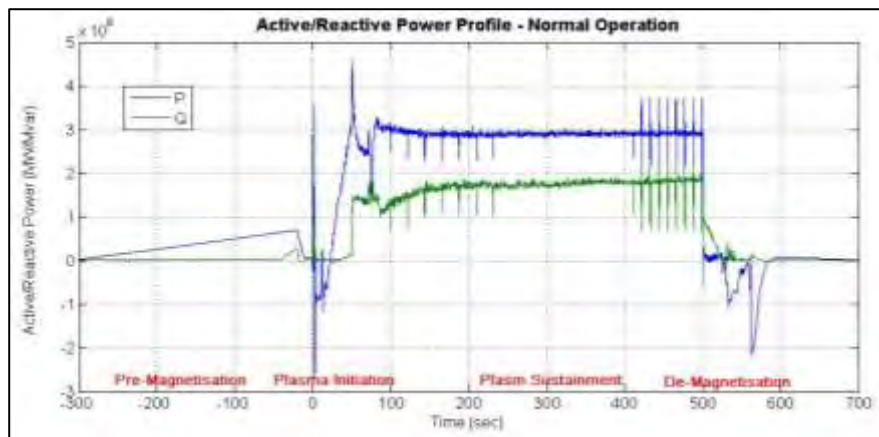


Fig. 1.13 PPEN expected power profile

In order to ensure the voltage stability in the 400 kV grid and reduced the harmonic distortion in PPEN, three 250 MVar Reactive Power Compensators (RPC) and Harmonic Filters (HF) units are connected, one to each of three 66 kV busbars. These are based on Static Var Compensator (SVC) technology comprising a Thyristor Controlled Reactor (TCR) and Harmonic Filters (HF). The present PPEN loads have been distributed between the three main step-down transformers in order to balance power and avoid getting transformers overloaded during plasma operation. The whole PPEN is capable to ensure that the system meets 400kV grid requirements and converges with the voltage regulation and harmonics distortion at 66kV and 22kV levels accepted by loads.

1.2.2 Steady State Electrical Network

The SSEN will receive up to 130 MW continuous power from the French 400 kV transmission network operated by RTE through two independent connectors, each capable of supplying the maximum load of the entire plant.

The normal operation voltage of the grid power source is 400 kV ± 5% at 50 Hz ± 1%. The grid power is then transformed to the 22 kV level by four, 2-winding, step-down transformers, each rated at 75 MVA, as per Fig.1.14. Rated load can be delivered with any one of the four step-down transformers out of service.

The emergency backup power will be generated by four diesel generators, two for safety and two for investment protection, each rated at 3.5 MW: these generators are connected to separate 6.6 kV busbars for supplying Class III (temporarily interruptible AC) power to the loads, which are safety or IP classified [17]. The loads with power requirements greater than 200 kW are supplied at the 6.6 kV level, through additional 22 kV/6.6 kV step-down transformers and 6.6 kV busbars of class IV and class III.

A capacitor bank for reactive power compensation is connected to each of the eight 6.6kV busbars to improve the power factor in nominal operating conditions to 0.93.

The remaining smaller loads will be connected to the 400/230 V network consisting of 14 transformer load-centre substations or load centres (LC).

The SSEN will provide AC power to several electrical loads: the major consumers are the cooling water and cryogenic systems requiring together about 80% of the total demand of 130 MW. About 13 MW - 8.7% of the total demand - must be provided even in case of a loss of off-site power: because of this autonomous diesel power generators will be used as backup during such events. Loads that cannot tolerate the 30 seconds of interruption time needed to start up the generators will be powered from AC or DC uninterruptible power supplies (UPS or CD chargers). This service, provided to safety or investment protection will be centralized; other interruptible supplies will be decentralized in order to optimize the design.

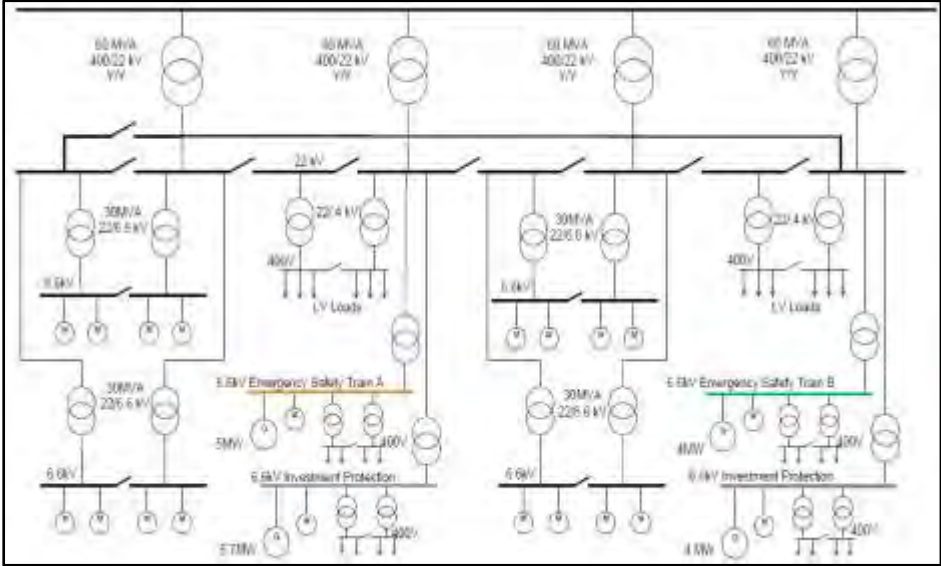


Fig. 1.14.SSEN Configuration

1.2.3 Reactive Power Compensation and Harmonic Filtering

The PPEN includes several AC/DC converters producing reactive power and harmonic currents at a higher level than acceptable to the French 400 kV transmission network. Therefore, a Reactive Power Compensator and

Harmonic Filtering (RPC&HF) system will be installed to reduce reactive power and the voltage distortion below the levels indicated in agreement between RTE and the Host (Agency ITER France). This RPC&HF system will be amongst the largest of its type installed in the world.

The RPC&HF units are connected to the 66 kV busbars (one unit for each busbar) and are based on Static Var Compensation (SVC) technology. In comparison with conventional SVCs, the ITER RPC&HF does not need the Thyristor Switched Capacitor (TSC) to generate inductive reactive power, thus providing cost reduction; these capacitor banks as harmonic filters are required to be permanently connected to the PPEN.

Taking account of the expected development of Thyristor Controlled Reactor (TCR) technology, the TCRs would be directly connected to the 66 kV busbars. Direct connection removes the need for TCR step down transformers. The disadvantage of this concept is that the 6-pulse operation of the TCRs will produce 5th and 7th harmonic currents and require corresponding harmonic filters. Nevertheless, the solution without TCR step-down transformer is the best choice for convenience and cost effectiveness.

A 200 - 250 MVar RPC&HF comprising a TCR and 6 LC filters is connected to each 66 kV busbar as shown in the one-line diagram in Figure 4.6

A 3D model of a typical 66 kV Thyristor Valve is shown in Fig. 1.15.

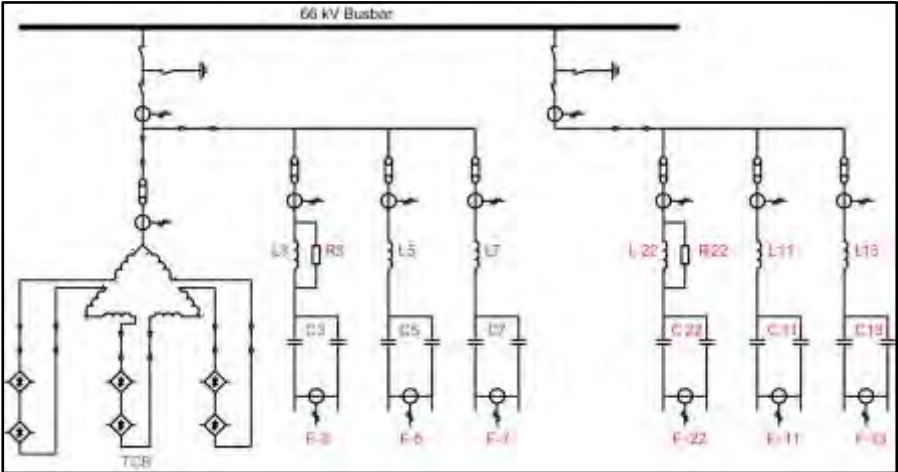


Figure 1.15 Single Line Diagram of a RPC & HF Unit

1.2.4 Coil Power Supplies

The Coil PS (Fig. 1.16) will include the following nine systems to supply controlled DC current to the TF and PF coils and the CS modules:

- One common PS for the 18 TF coils;
- One common PS system for the CS1 upper and lower modules connected in series;
- Four PS systems for the CS2 upper, CS2 lower, CS3 upper and CS3 lower modules;
- Two PS systems for individual supply of the PF1 and PF6 coils;

- One common system for the four outer PF coils, i.e. PF2, PF3, PF4 and PF5, used for plasma vertical stabilization.

In addition, nine relatively small PS systems with very similar configurations will supply the flux error Correction Coils (CCs).

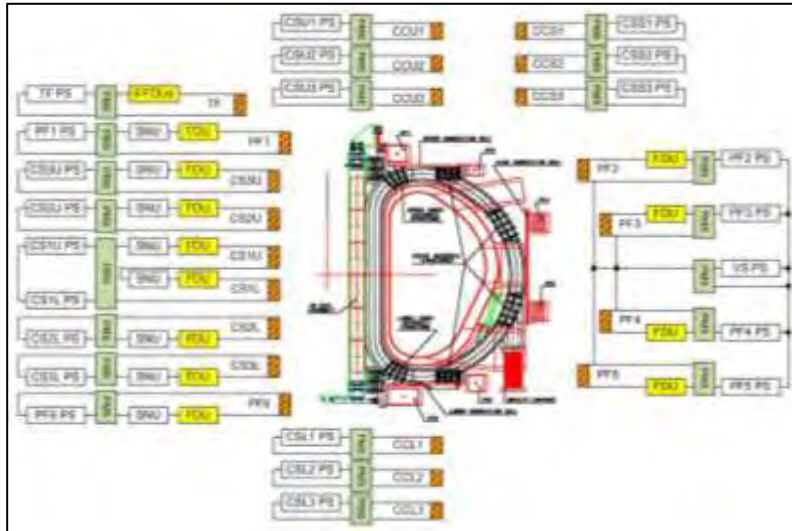


Fig. 1.16 Configuration of Coil Power Supplies

1.3 Cryogenic System

Cryogenics is the branch of physics and engineering that deals with very low temperatures that do not naturally occur on Earth (the word cryos - κρύο - is Greek and means "icy cold"): at ITER the cryogenic technology will be extensively used to create and maintain low temperature conditions (3.7 K, -270° C) for the magnet, vacuum pumping and some diagnostics systems, and it will produce the required cooling power and distribute it through a complex system of cryolines and cold boxes that make up the cryo-distribution system.

It is the second most important system inside the plant with 41 MW required for the operation, second only to the Cooling Water system (almost 80 MW).

Consider that the large pulsed heat loads are deposited in the magnet system due to electromagnetic field variation and nuclear heating: for example, an instant value of the nuclear heating during the plasma burn phase is close to 14 kW for a fusion power of 500 MW, so the total heat deposition due to AC and eddy current losses is about 13 MJ for one plasma pulse.

It is easy to understand that a refrigerator system is necessary to operate the fusion process.

The cryogenic system must operate over a wide range of ITER plasma scenarios, such as the 400 seconds plasma pulses with the fusion power of 500 MW, the extended plasma pulses with an enlarged plasma burn phase of 1000 seconds and 3000 seconds for the fusion power of 400 MW, short plasma pulses with an enlarged fusion power of 700 MW.

The ITER cryoplant is composed of helium and nitrogen refrigerators combined with an 80 K helium loop. Storage and recovery of the helium inventory (25 tons) is provided in warm and cold (4 K and 80 K) gaseous helium tanks:

- Three helium refrigerators supply the required cooling power via an interconnection box providing the interface to the cryo-distribution system;
- Two nitrogen refrigerators provide cooling power for the thermal shields and the 80 K pre-cooling of the helium refrigerators. The ITER cryogenic system will be capable of providing cooling power at three different temperature levels, i.e. 4 K, 50 K and 80 K.

The distribution of cooling power is accomplished through cryo-distribution boxes with helium circulating pumps for the cooling of the magnets and cryo-pumps, and a complex system of cryogenic transfer lines located both within the Tokamak Building, within the Cryoplant buildings, and between the two.

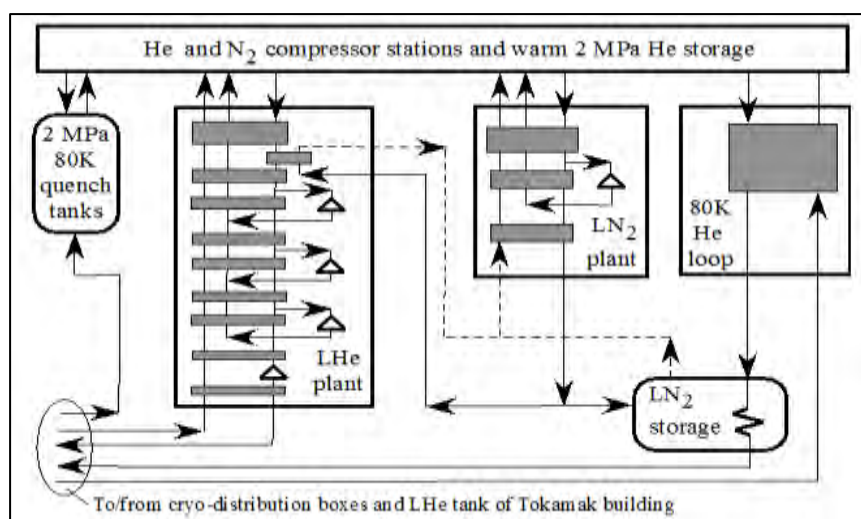


Fig. 1.17 Principal arrangement of ITER cryogenic plant

The ITER cryogenic system will be the largest concentrated system in the world with an installed cooling power of 65 kW at 4.5 K (helium) and 1300 kW at 80 K (nitrogen). After the Large Hadron Collider at CERN, it is the largest cryogenic system ever built. The design of the ITER cryogenic system was validated during tests at existing facilities around the world [19] [20].

This information is useful to understand the explanations in the following chapters: the analyses of the effects caused by the variation of voltage were all made on MV motors whose loads are compressors or pumps operating for the cryogenic system. It is very important to understand that possible electrical disturbances cannot be considered as just electric problems, but they are linked to the load side: in fact a variation of voltage can change the speed of the MV motors and if this speed is not in the tolerance of the motor it could be required to stop the operation of the fusion plant for several hours, so with consequences for the production and financial losses, since during this time no power would be generated and no energy would be sold.

Electrical circuit and its load sides must be considered together, since one affects the other and vice versa.

2. User Guide for ETAP and SimPowerSys

This chapter will give some useful information regarding the two programs used for the studies described in the following.

2.1 General Information

The most part of the analyses done at ITER are based on two different software, i.e. ETAP and Matlab Simulink: these programs are very different but both can offer the possibility to create complex systems, ETAP just for electrical studies and Matlab Simulink for many other fields, such as electronics, mechanics, hydraulics.

Following an extensive use of these software packages, I have developed some knowledge and experience useful to be shared, especially about the passage from one to the other and vice versa: consequently, the aim of the following paragraphs is to describe this type of information and, at the same time, to introduce some aspect of the works done.

2.2 ETAP

ETAP is a graphical electrical power system analysis program designed and developed for engineers to manage the diverse discipline of power systems in one integrated package with multiple interface views such as AC and DC networks, lines, panels.

It has a quite large and comprehensive library of AC and DC electrical components for power distribution and consumers; inside the various elements available, ETAP combines the electrical, logical, mechanical aspects of systems in a unique database: for example, for a cable there is the possibility to underline the electrical properties, the physical dimensions, but also some information regarding the raceways [21].

ETAP has a user face relatively simple and this allows to quickly build up a model to be analysed.

There are also several modules useful to study different scenarios, always with elasticity but according to the standards. The modules mainly used in the following analyses are the *Short Circuit*, *Motor Starting* and *Transient Stability*.

The solver is basically in the frequency domain and therefore it cannot be used for transients shorter than the period of the fundamental AC frequency.

ETAP 12.5 and 12.6 are the versions used for the studies made.

2.3 Matlab Simulink – SimPowerSys

Matlab is well known to be a numerical computing environment which allows matrix manipulation, plotting functions and data, implementation of algorithms and other options. It is intended primarily for numerical computing and so Simulink is introduced as an additional package to implement graphical multi-domain simulations [22].

Simulink has as primary interface a graphic block-diagramming tool and a very large library with a customizable set of blocks. Inside its libraries there are many toolboxes, each one useful for diverse fields of studies, such as electronics, mechanical and electrical systems: one of these toolboxes is SimPowerSys, which is suitable for electric studies and, in fact, most of the following analyses are made with it.

SimPowerSys has a vast library, larger than the one in ETAP, and this aspect allows to build very detailed and custom-made models and to reproduce a bigger number of scenarios: sometimes there is the possibility to analyse situations not reproducible with ETAP. This is one the reason why some study has been made using SimPowerSys instead of ETAP.

It also has different solvers, including one in the time domain useful to study fast transients.

The version used is R2014a.

2.4 Input data for Electrical Motors

The differences between ETAP and SimPowerSys are not only in the available blocks inside the libraries or in the solver: in fact, sometimes the same element could have a diverse way to fill the input data and this aspect could develop irregularities when there is the transfer from one program to the other. The difficulties could be due to the fact that some input data is not directly provided in the datasheet or this latter could give precise details but not the ones needed.

For this reason, in the following paragraphs are described some of the problems that could be faced during the use of both ETAP and SimPowerSys and with the solutions to use; the attention is paid on the electrical motors and the transformers, since they are the most used elements in the equivalent scheme built for the analyses performed.

2.4.1 ETAP Specifications

In ETAP the motor block allows to describe the machine in a very complete way, but to do it several details are required from the manufacturer. Inside the block there are different entry fields:

- *Nameplate, Impedance* and *Inertia*, where data like power (kW), efficiency (%), power factor (%), mechanical details such as torque (Nm) and inertia ($\text{kg}\cdot\text{m}^2$) have to be inserted;

- *Load*, where it is possible to select the load curve between one of those proposed or others custom-made;

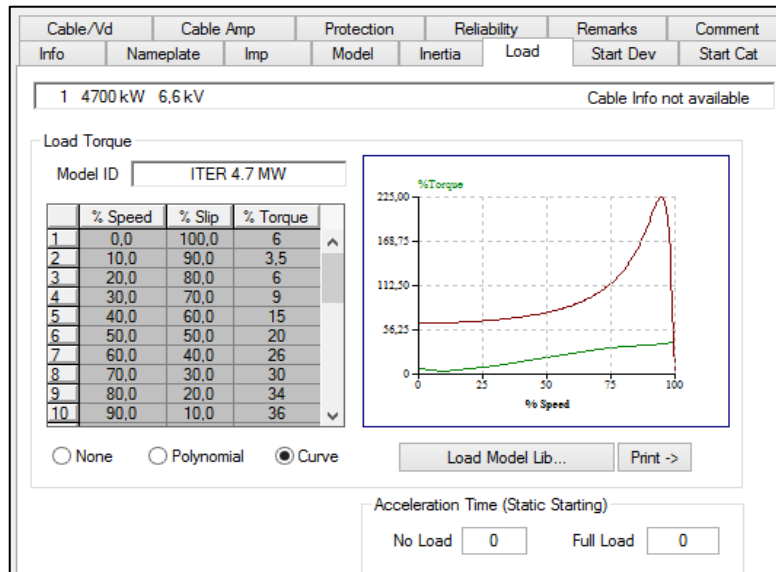


Fig. 2.1 ETAP Motor Block – Load

- *Model*, where it is described the electrical circuit of the motor and the consequent torque-slip characteristic;

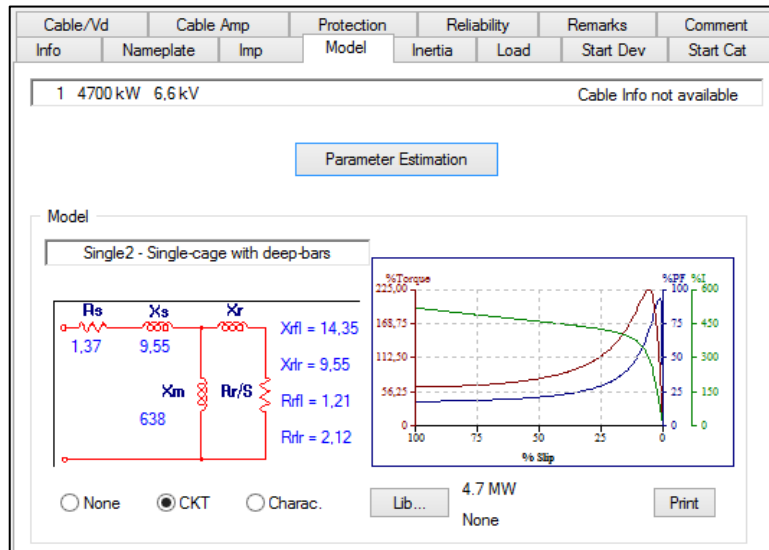


Fig. 2.2 ETAP Motor Block – Model

The parameters indicated in Fig. 2.2 are the following:

R_s	Stator resistance
X_s	Stator reactance
R_{rfl}	Rotor resistance at full load
R_{rr}	Rotor resistance at locked rotor
X_{rfl}	Rotor reactance at full load
X_{rr}	Rotor reactance at locked rotor

X_m	Magnetizing reactance
-------	-----------------------

Tab. 2.1

All these values should be provided by the manufacturer and in ETAP are in *per unit* (p.u.), expressed in percentage. Rotor resistance and reactance are referred to the stator.

The p.u. impedance is defined as follows:

$$Z_{pu\%} = \frac{Z_{abs}}{Z_{base}} \cdot 100 \quad [2.1]$$

$$Z_{base} = \frac{V_r}{\sqrt{3} \cdot I_r} \quad [2.2]$$

Where

- Z_{abs} is the magnitude of the impedance [Ohm];
- V_r is the rated voltage [V];
- I_r is the rated current [A].

2.4.2 SimPowerSys Specifications

In Simulink there is the possibility to choose between motors with SI Units or p.u.: since the motors used in the analyses need to have as input the load-speed characteristic, it was decided to use the SI Units in order to avoid mistakes creating the curves. The biggest differences between the two programs are that SimPowerSys makes the distinction between stator and rotor impedance and moreover there is no reference to the locked rotor and full load conditions, as shown in Fig. 2.3.



Fig. 2.3 SimPowerSys Asynchronous Motor Block

Since in ETAP the values are all in percentage of p.u, in SimPowerSys it is necessary to convert them in Ohm in order to fill correctly the spots.

The following formulas describe the way to pass from the p.u values of ETAP to the SI Units of SimPowerSys for an asynchronous motor with a squirrel cage.

- a) Calculate the base impedance as shown in [2.2];
- b) Take the p.u. values [Tab. 2.1] and multiply the for Z_{base} in order to get Ohm as unit:

$$R_s = Z_{base} \frac{R_s \text{ pu}}{100} \quad [2.3]$$

$$X_s = Z_{base} \frac{X_s \text{ pu}}{100}$$

$$R_{RS} = Z_{base} \frac{R_{Rlr} \text{ pu}}{100}$$

$$X_{RS} = Z_{base} \frac{R_{Rlr} \text{ pu}}{100}$$

$$X_m = Z_{base} \frac{R_{Spu}}{100}$$

Where

- R_s is the stator resistance [Ohm]
- X_s is the stator reactance [Ohm]
- R_{RS} is the rotor resistance seen from the stator [Ohm]
- X_{RS} is the rotor reactance seen from the stator [Ohm]
- X_m is the magnetizing reactance [Ohm]

These are the values to use in SimPowerSys. Fundamental for the calculations are the rated voltage and current, since they determine the Z_{base} which allows the conversion.

For example, taking the data of Tab. 2.2 and using formulas [2.2] [2.3], the impedance will be as follows:

V_n [V]	6600
I_n [A]	122
R_s [% p.u]	0.724
X_s [% p.u]	13.919
R_{rtr} [% p.u]	1.575
X_{rtr} [% p.u]	2.72
X_m [% p.u]	474.2

Tab. 2.2

$$Z_{base} = \frac{6600}{\sqrt{3} \cdot 122} = 31.2337 \text{ } [\Omega]$$

$$R_s = 31.2337 \cdot \frac{0.724}{100} = 0.22613 \text{ } [\Omega]$$

$$X_s = 4.34742 \text{ } [\Omega]$$

$$R_{RS} = 0.492 \text{ } [\Omega]$$

$$X_{RS} = 0.8495 \text{ } [\Omega]$$

$$X_m = 148.110 \text{ } [\Omega]$$

2.5 Input data for Transformers

As done for the motors, also the differences regarding the transformers in the two programs will be described, focusing again the attention on the way to convert the impedances.

2.5.1 ETAP Specifications

The transformers can be well described in ETAP since there are several voices to fill: in fact, there is the possibility to precise all the standard parameters such as the short circuit impedance ($Z_{\%}$), the rated voltages, the rated power (S_n), the windings connection, the isolation and also something about the working conditions (altitude, ambient temperature).

The voices regarding the impedance are easy to complete, because once the $Z_{\%}$ and the ratio X/R (the parameters typically provided) are set then all the other data are directly calculated by ETAP.

Reliability		Remarks			Comment		
Info	Rating	Impedance	Tap	Grounding	Sizing	Protection	Harmonic
35 MVA IEC Liquid-Fill ONWF/ONAN 65 C						22 6,6 kV	
Impedance		Z Base					
	%Z	X/R	R/X	%X	%R	MVA	
Positive	11	30	0,033	10,994	0,366	35	
Zero	11	30	0,033	10,994	0,366	ONWF/NAN 65	
		Typical Z & X/R		Typical X/R			

Fig. 2.4 ETAP Transformer Block - Impedance

Again, the values for the resistance (%R) and reactance (%X) are expressed in percentage of p.u.

2.5.2 SimPowerSys Specifications

The differences between the two programs are almost the same seen with the asynchronous motors, because in SimPowerSys there is

- The possibility to use SI Units;
- The distinction between primary and secondary winding and not a unique compact value.

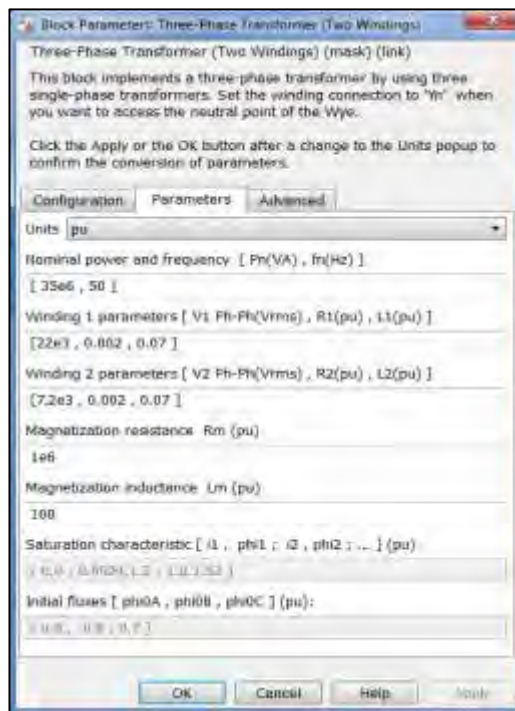


Fig. 2.5 SimPowerSys Transformer Block

The following formulas show how to fill the correct parameters in a transformer block, both in p.u. and SI Units.

1) Per Unit

In p.u. it is sufficient to take “compact” value of the resistance and reactance in ETAP and divide them by 2:

$$R_{SPS} = \frac{R_{ETAP}}{2 \cdot 100} \quad [2.4]$$

$$X_{SPS} = \frac{X_{ETAP}}{2 \cdot 100}$$

Where

- R_{SPS} and X_{SPS} , are the resistance and reactance [p.u] in SimPowerSys;
- R_{ETAP} and X_{ETAP} , are the resistance and reactance taken from ETAP [p.u.].

These are the values to be used in both the windings and the reason will be clear with the description of the formulas for the SI Units transformer.

2) SI Units

- a) Calculate the base impedances for the two windings (subscript 1 is referred to the primary, 2 to the secondary):

$$Z_{base1} = \frac{V_{r1}^2}{S_R} \quad [2.5]$$

$$Z_{base2} = \frac{V_{r2}^2}{S_R}$$

S_R is the rated power (VA).

- b) Evaluate the resistance and reactance in the windings using R_{SPS} , X_{SPS} and Z_{base} from [2.4] [2.5]:

$$R_1 = Z_{base1} \cdot R_{SPS} \quad [2.6]$$

$$X_1 = Z_{base1} \cdot X_{SPS}$$

$$R_2 = Z_{base2} \cdot R_{SPS}$$

$$X_2 = Z_{base2} \cdot X_{SPS}$$

The results from [2.6] are the values to use in the transformer block, remembering to convert the reactance in inductance.

To bring R_2 and X_2 from the secondary to the primary do as follows:

$$R_{12} = R_2 \cdot \frac{V_{r1}^2}{V_{r2}^2} \quad [2.7]$$

$$X_{12} = X_2 \cdot \frac{V_{r1}^2}{V_{r2}^2}$$

The magnitude of the total impedance of the transformer seen from the primary is the following:

$$Z_{tot} = \sqrt{(R_1 + R_{12})^2 + (X_1 + X_{12})^2} \quad [2.8]$$

It can be easily verified that

$$Z_{\%} = \frac{Z_{tot}}{Z_{base1}} \cdot 100 \quad [2.9]$$

For example, consider the data in Tab. 2.3:

V_{r1} [V]	22000
V_{r2} [V]	6600
$Z_{\%}$	11
X/R	30
S_r [MVA]	35
R_{ETAP} [%]	0.366
X_{ETAP} [%]	10.994

Tab. 2.3

For the transformer in p.u. it will be as follows:

$$R_{SPS} = \frac{0.366}{2 \cdot 100} = 0.00183 \text{ [p. u]}$$

$$X_{SPS} = \frac{10.994}{2 \cdot 100} = 0.05497 \text{ [p. u]}$$

According to formulas [2.4]-[2.9], the equivalent values in SI units are these:

$$Z_{base1} = \frac{22000^2}{35 \cdot 10^6} = 13.8285 \text{ } [\Omega]$$

$$Z_{base2} = \frac{6600^2}{35 \cdot 10^6} = 1.24457 \text{ } [\Omega]$$

$$R_1 = 13.8285 \cdot 0.00183 = 0.025306 \text{ } [\Omega]$$

$$X_1 = 0.76015 \text{ } [\Omega]$$

$$R_{12} = 0.025306 \text{ } [\Omega]$$

$$X_{12} = 0.76015 \text{ } [\Omega]$$

$$Z_{tot} = 1.5211 \text{ } [\Omega]$$

$$Z_{\%} = 11 \text{ } \%$$

The short circuit impedance corresponds to the one given in Tab. 2.3, showing the correctness of the formulas.

3. Input Data

In this chapter there is some useful information regarding the MV motors and other elements taken into account in the following analyses.

3.1 MV Busbars JB-3000 and JB-4000

Before going into the details of the studies made, it is important to give some information on what I have undertaken in order to put in the right context and understand the analyses performed.

As shown in Fig. 1.14, the Steady State Electrical Network is made by many busbars at different voltages (22 kV, 6.6 kV and 400 V), each one with its loads (especially motors) and connected with a precise system of the fusion plant (cooling water, cryogenic system or others): in the following studies the attention is on the motors of two 6.6 kV busbars, individually identified in the ITER Network as 43ALM1-JB-3000 and 43ALM1-JB-4000 and together as MV-01. This portion of the Network is dedicated to the cryoplant and it is shown in Fig. 3.1.

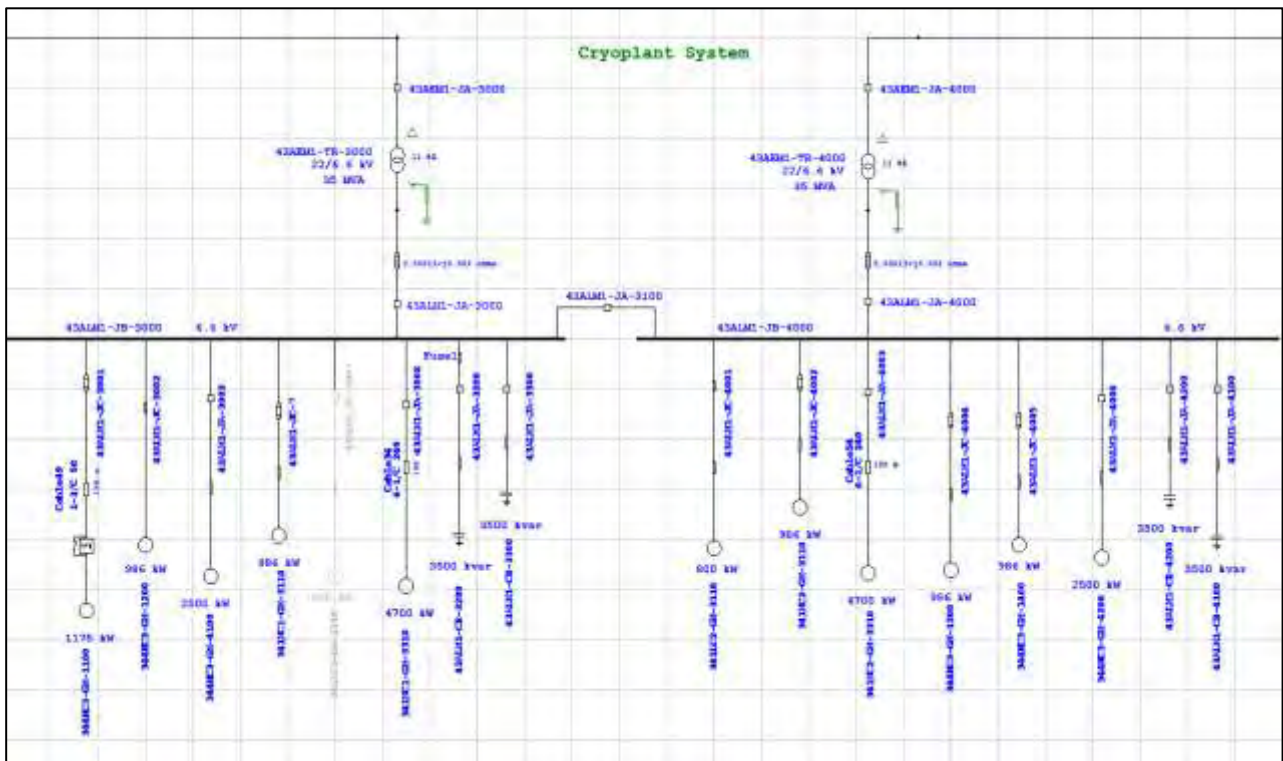


Fig. 3.1 JB-3000 and JB-4000 busbars

These busbars can work in two different configurations, i.e. coupled or uncoupled: in normal conditions they will not be connected through the circuit breaker (43ALM1-JA-3100).

The power will be provided by two three-phase transformers, whose main data are in Tab. 3.1.

Transformers	43AEM1-TR-3000	43AEM1-TR-4000
V _{1r} [kV]	22.0	22.0
V _{2r} [kV]	6.6	6.6
S _r [MVA]	35	35
Z _{cc} [%]	11	11
Connection	Dyn11	Dyn11

Tab.3.1

The minimum short circuit power on the two busbars, calculated when they are not coupled and following the IEC 60909 standards, is around 305 MVA ($I_k = 26.9$ kA).

The motors have different characteristics, not only for the electrical data but also for the type of load connected: more details about these motors are in the following paragraphs.

Note that some of the values reported could see some change because currently they are still not the final ones: this means that the results obtained from the analyses performed will be different in case of future upgrades of the data.

What is currently certain is the type of mechanical load that will be connected to each motor, i.e. centrifugal or screw compressor.

Centrifugal compressors are continuous flow machines in which one or more rotating impellers accelerate the gas when it passes through them; the high kinetic energy obtained is then converted in static pressure by slowing the flow with a diffuser. They are typically used when a large flowrates is needed and in the ITER cryogenic plant they will compress nitrogen.

A screw compressor uses a rotatory type positive displacement mechanism with two meshing helical screws, better known as rotors, to compress the gas: in fact, rotating twin rotors work as the pistons in the centrifugal compressor. In this way the compression is done continuously by the rotation of the rotors. Screw compressors are suitable to produce large volumes of high-pressure gas and in the cryogenic system they are used to work on helium. There are two types of screw compressor technologies, i.e. with and without oil flooded: the IO Cryogenic team selected the first one because the use of oil allows to increase the efficiency of the helium compressed.

The identification code used is useful to understand which type of compressor is connected to the MV motors of Fig. 3.1: the letter “N” indicates nitrogen, while letter “H” helium. Note also that the tag “LC” is referred to compressors working on helium, in this case on the 80 K loop.

3.2 LN2 GAN Motors Data

The 4.7 MW three-phase squirrel cage asynchronous motors connected to busbars JB-3000 and JB-4000 are the biggest ones inside the ITER Network and they play an important role due to their load: they are both coupled with a centrifugal compressor useful to produce liquid nitrogen (LN2) and gaseous nitrogen (GAN) which will be used in two refrigerators to provide cooling power for the thermal shields and in the 80 K pre-cooling of the helium refrigerators of the cryogenic plant. If the motors stop to operate, all the refrigeration process will be lost and therefore there will be no possibility to maintain the low temperature conditions for

the magnet, vacuum pumping and some diagnostics systems: in this situation the entire fusion plant has to be stopped and before being able to work again it will take several hours.

3.2.1 Main Data

According to the manufacturer documents, the general data are the following:

LN2 GAN Motors	341NC1-GM-3310	341NC2-GM-3310
Busbar	43ALM1-JB-3000	43ALM1-JB-4000
Power [kW]	4700	4700
Rated Voltage [V]	6600	6600
Rated Frequency [Hz]	50	50
Rated Speed [rpm]	2972	2972
Nr of poles	2	2
Efficiency [%]	96.5	96.5
Power Factor	0.89	0.89
Rated Torque [Nm]	15103	15103
Rated Current [A]	478.7	478.7
Motor Inertia [kg·m²]	80	80
Driven Inertia [kg·m²]	169	169

Tab. 3.1

3.2.2 Electrical Model

Following the definitions given in Tab. 2.2, the electrical model used for these motors is the following:

R_s [p.u]	0.0137
X_s [p.u]	0.0955
R_{rlr} [p.u]	0.0212
R_{rl} [p.u]	0.0112
X_{rlr} [p.u]	0.0955
X_{rl} [p.u]	0.1435
X_m [p.u]	6.38

Tab. 3.2

3.2.3 Load Model

Torque and current diagrams are also available for the LN2 GAN motor load.

Speed [%]	Slip [%]	Torque [%]
0	100	6
10	90	3.5
20	80	6
30	70	9
40	60	15

50	50	20
60	40	26
70	30	30
80	20	34
90	10	36
100	0	39

Tab. 3.3

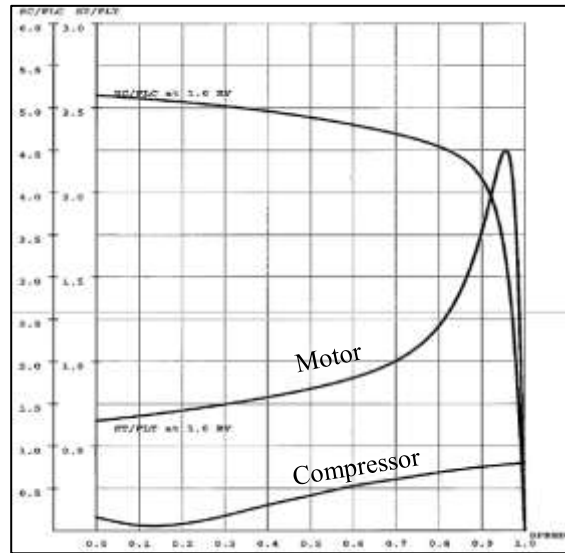


Fig. 3.2 LN2 GAN torque and current

3.3 LN2 and LHe Motors Data

In the following tables are shown the main data of the other three-phase asynchronous motors connected to busbars JB-3000 and JB-4000. Note that:

- Motor 341LC1-GM-3110 (800 kW) is not included since no precise value is available;
- The 1175 kW motors have a different power (1100 kW): this difference is due to some inaccuracy in the actual information, especially regarding the impedance. Anyway, the main data of these motors are very close;
- 341NC1-GM-3110 and 341NC2-GM-3110 motors in Fig. 3.1 are indicated with a power equal to 986 kW, but in the reality they will have 978 kW: this change is due to the lack of information about the correct machine and so it was decided to use the same values of the one with 986 kW. Consider that the correct motors will be connected to centrifugal compressor and not to a screw compressor like the 986 kW motor.

3.3.1 Main Data

Note that *total inertia* is the sum of motor and driven inertia.

Power [kW]	Rated Voltage [V]	Frequency [Hz]	Rated Current [A]	Rated Speed [rpm]	Rated Toque [Nm]	Nr. of Poles	Tot. Inertia [kg·m ²]
2500	6600	50	248	2987	7992	2	44.6
1175	6600	50	122	2985	3759	2	23.3
986	6600	50	98.9	2969	3172	2	23.2

Tab. 3.4

3.3.2 Electrical Model

The values are expressed in p.u (%):

Motor	R_s	X_s	R_{rlr}	R_{rfl}	X_{rlr}	X_{rfl}
2500	0.755	12.325	1.72	0.416	7.396	11.44
1175	0.724	13.919	1.575	0.49	2.72	2.959
986	0.817	11.29	9.29	1.023	7.137	2.57

Tab. 3.5

3.3.3 Load Connected

The following table summarize which loads are connected to the motors.

Motor	Compressor	Gas Compressed
2500	Screw	He
1175	Screw	He
986	Screw	He
978	Centrifugal	N2

Tab. 3.6

4. Motor Starting Analysis

In this chapter are described the analyses and the results regarding the LN2 GAN motor starting process in order to foresee the consequent impact on the voltage.

4.1 Starting Methods for Induction Motors

The starting of a three-phase asynchronous motor for applications which does not require to change the speed can be obtained in several different ways, according to the modality of the application of the voltage across the stator windings and also to the electrical and mechanical parameters which characterize the machine. The major concern regarding the starting process of an induction motor is the high inrush current, caused by the fact that the motor at the beginning has no load connected and, seen from the electrical point of view, this situation looks like a short circuit.

The choice of the best suitable starting process is dependent on the application (load connected, torque required) and eventually the economic aspects as well.

The simplest and perhaps most traditional method is the *Direct on Line* starting (abbreviated as DOL) and consists in connecting the motor directly to the electrical network, so to the full supply voltage. The main problem linked to this process is the inrush current, which can reach values around 10-12 times the rated one in the first instants and then it can decrease to 6-8 times: the effects of this current are the high electrodynamic stresses on the motor, both on the windings and the body of the machine. Moreover, if the motor has a high power, there is also the problem of voltage drops on the supply grid that could create negative impacts on other possible loads connected besides the motor itself. This brings typically to use the DOL method with small power motors.

Considering the problems with the DOL technique, other methods could be used in order to reduce the starting current: the better solution is to apply a reduced voltage to the motor, because this can limit the inrush current but unfortunately also the torque. The most common types of starting process which allow to apply the mentioned voltage reduction are those that use star-delta transitions on the windings, or autotransformer, or a connection of stator resistors and/or reactors or specific electronic devices such as inverter and soft starter.

- The star-delta (Y/ Δ) starting is the most known and commonest starting system to reduce the voltage: it consists in connecting by first the stator windings in star configuration (Y) and then, after that the motor reaches a precise speed, the connection is changed into the delta configuration (Δ). It is suitable when the motor starts with no load connected or when the load torque is low and constant;
- With the autotransformer starting the reduction is obtained changing the position of the tap in order to modify the transformation factor (k) between the primary and secondary voltage. At the

beginning, the motor receives a precise voltage which is then reduced through the tap-changer. Starting with the autotransformer is more expensive than the Y/ Δ process and typically it is used with medium and high power motors with a big inertia;

- Connecting before the motor resistors or reactors in series to the stator is another way to reduce the voltage: the total impedance is higher at the beginning and this enables to contain the inrush currents. When the acceleration phase is finished, the reactors and resistors are disconnected and the motor is directly connected to the supply point;
- A modern and alternative method is based on the use of electronic static devices: they control the starting process, to limit the inrush current and to set the total time, so making the starting process softer than previous ones. On the other hand, this method requires a high initial investment. A soft starter and the frequency inverter are two of the most used possibilities: the following paragraph gives some information regarding the soft starter, since it is the device connected to the 4.7 MW motors.

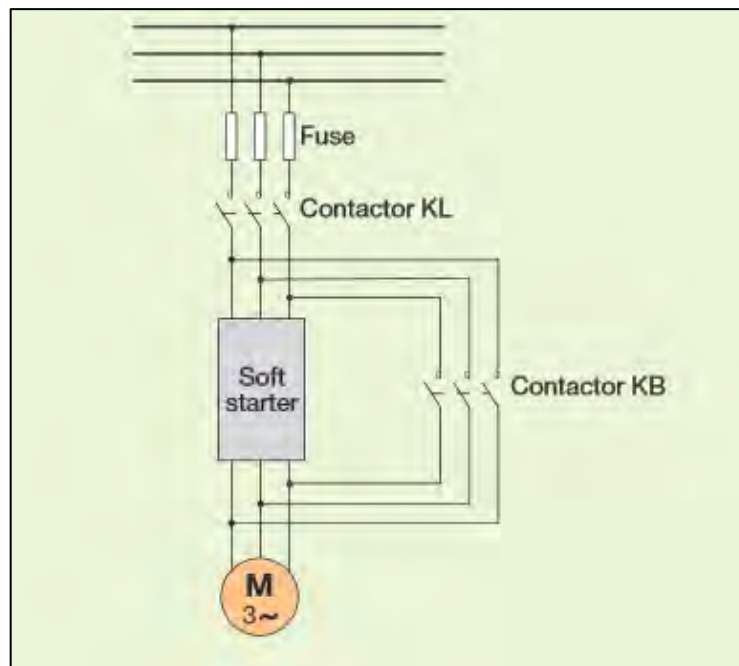


Fig. 4.1 Soft Starter Connection

4.1.1 Soft Starter

This electronic device provides a remedy to the problems described: in fact, producing a continuous increase of the voltage (and so of the torque) it gives the possibility for a selective reduction of the inrush currents. The motor voltage is slowly ramping-up within a precise period (see Fig.4.4), which has to be the most suitable for the connected motor.

The voltage at the motor terminal bus is changed with a phase angle control of the sinusoidal half wave, as shown in Fig. 4.2: two thyristors are connected in each phase in anti-parallel, so one is for the positive half wave and the other one for the negative half wave.

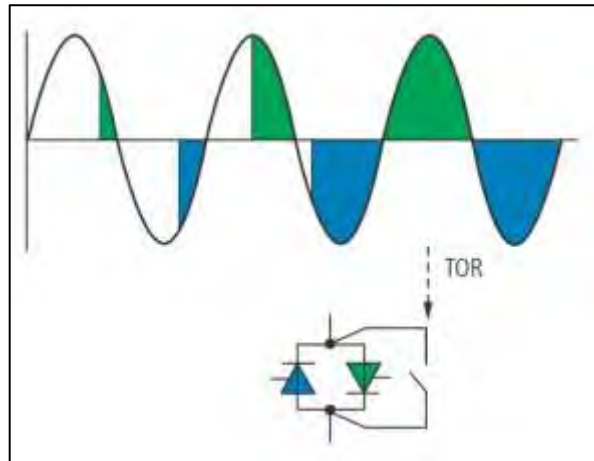


Fig. 4.2 Phase Angle Control and By-pass Contact

The effect of the thyristors control on the voltage and the power is shown in Fig. 4.3: the voltage is available only during a period equal to theta (θ) during the semi-waves and therefore the magnitude can be different according to the value of this conduction angle.

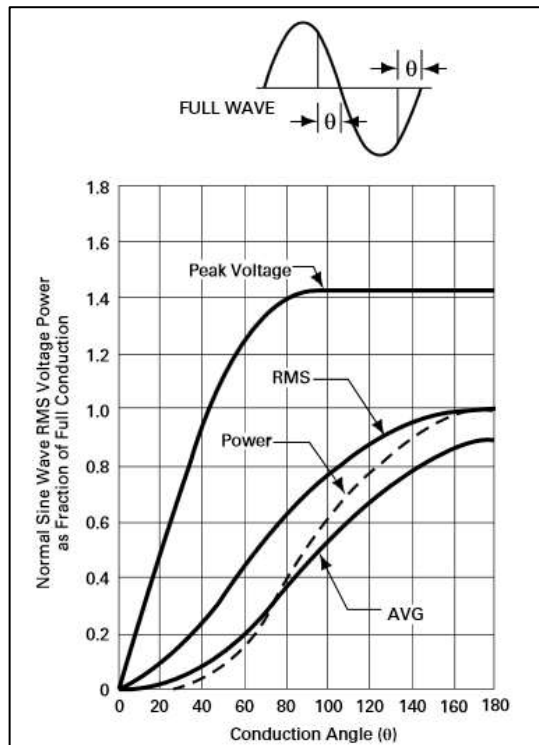


Fig. 4.3 Voltage RMS and Power

After that the time of ramp (TOR), i.e. the starting time set, is completed the thyristors are fully controlled in the semi-period ($\theta = 180^\circ$) and then the soft starter could be bypassed, so leaving the motor directly

connected to the supply grid. The losses in the soft starter can be reduced by using a lower contact resistance in the mechanical switching contacts [23].

The acceleration time results from the setting of the starting voltage (U_{start}) and the time of the ramp (t_{start}): these two parameters determine the progression of the voltage applied to the motor terminal bus and therefore of the inrush current. In the process the current rises to its maximum values and then falls down to the rated one after that the motor rated speed is reached. Note that a maximum limit for the current can be set and it can be different from the value in DOL.

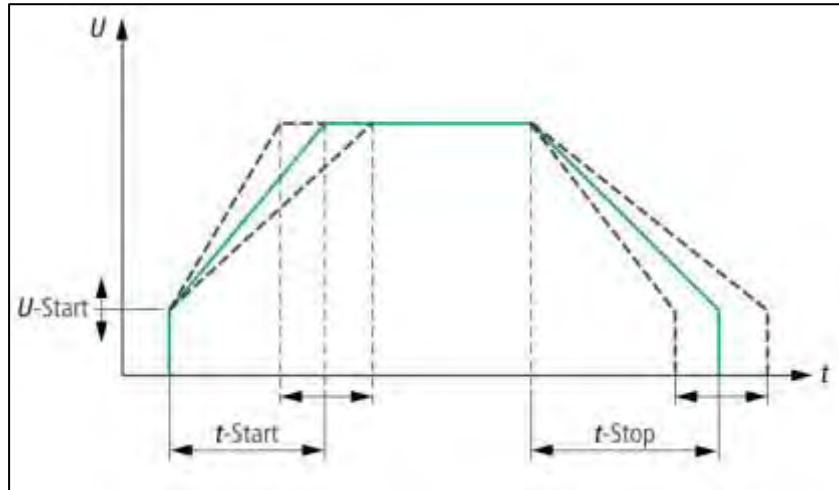


Fig. 4.4 Voltage RMS Curve in a Soft Starter

Unlike the other starting techniques described, a soft starter gives also the possibility to control the slowdown of the motors: the set stopping time (t_{stop}) must be longer than the natural one that occurs without the soft starter (and the load connected).

Both the starting and stopping process depends on the mechanical load coupled.

This description of the soft starter is useful to understand better some of the choices made in the following analyses, since this device has been used in connection with the LN2 GAN motor.

4.2 Motor Starting Study

The aim of this study is to perform an investigation of the starting process of the LN2 GAN motor in different scenarios considering the use of a soft starter. The analyses are based on the last CAPSIM's study regarding the same starting process but without the soft starter connected to the motor: in fact, this is a sort of continuation of what was done before and therefore, to highlight the differences between the different configurations, it followed the same principles in the settings of the analyses.

Note that between the last CAPSIM's study and this one there are many differences in

- The data of the MV motors of busbars JB-3000 and JB-4000;

- The motor disposition in the busbars;
- The mechanical loads, connected since now some information is available.

The reason why the soft starter is needed in the system is very clear looking at Fig. 4.5: with the 4.7 MW motor started in DOL the voltage drop is almost 15% of the rated one and so very close to the limit authorized at the motor terminals (the minimum start-up voltage is 85%), therefore it is easy to understand that this impact must be reduced. Considering that this motor will see several starting processes during the tests that ITER will perform, it becomes important containing the drops in order to minimize the problems on the supply grid.

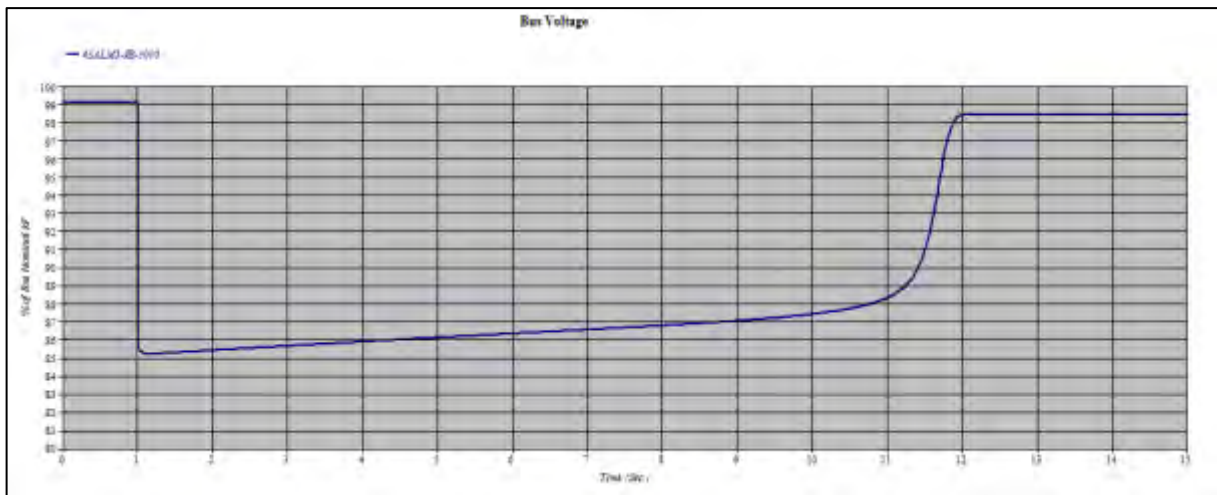


Fig. 4.5 Voltage Drop at the motor terminal with DOL starting

Location	Voltage BEFORE Starting [%]	Voltage DURING Starting [%]	Voltage AFTER Starting [%]	Duration [s]
43ALM1-JB-3000	99.75	85.24	98.45	11

Tab. 4.1

The studies are made with ETAP and in part with SimPowerSys in order to compare the results.

4.2.1 Criteria to Respect

In order to estimate the voltage drop of the LN2 GAN motor with the soft starter in the worst conditions, the following criteria are considered:

- The minimum 400 kV off-site short circuit power (3.6 GVA) is assumed;
- 400 kV off-site voltage of 94% (pulse influence on 400 kV grid is not taken into consideration, as per SRD-43 (v3.1));
- The minimum startup voltage authorized at the motor terminals is 85% of their rated voltage;

- Limit of voltage variations for the 6.6 kV power, including the transients that are produced by motor starting is $\pm 8\%$.

Note that the capacitor banks are connected when all motors are connected, so there is no capacitor bank when the 4.7 MW motor studied is the first one to be started [25].

4.2.2 Starting Scenarios

In order to have a complete overview of the impact on the voltage drop, four different scenarios are taken into account, following the same setting used in the CAPSIM's report.

a) Normal Study Case

It is considered that LN2 GAN motor is the first one to be started and the two 22/6.6 kV transformers are both in service, with JB-3000 and JB-4000 busbars not coupled.

No capacitor bank is connected.

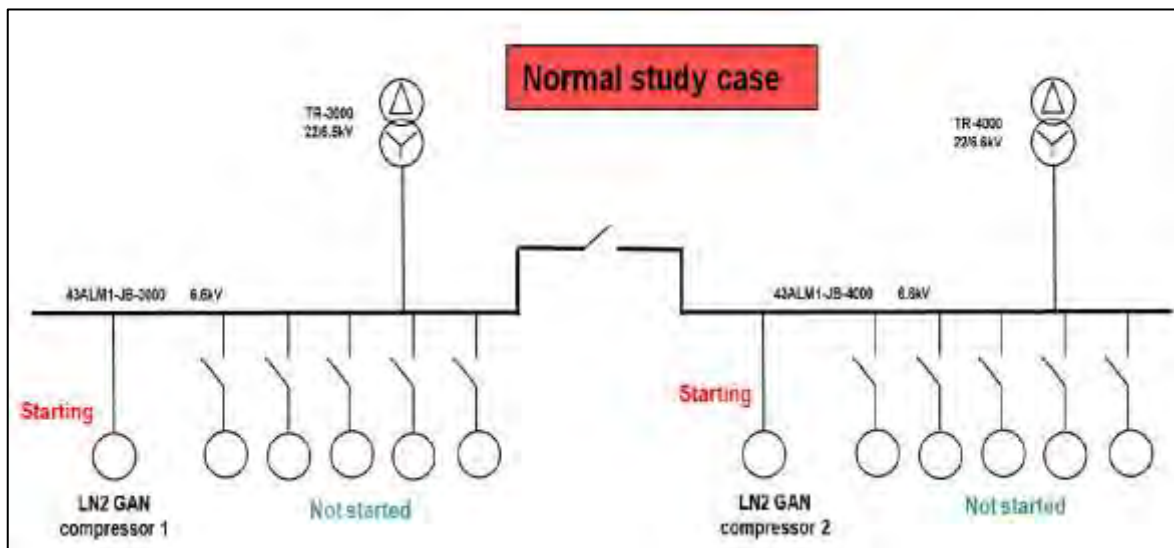


Fig. 4.6 Normal Study Case Configuration

b) Intermediate Study Case

LN2 GAN motor is the last one to be started, so after all the other MV motors have already completed the starting process. The two 22/6.6 kV transformers are on service and the busbars are not coupled.

All the capacitor banks are connected.

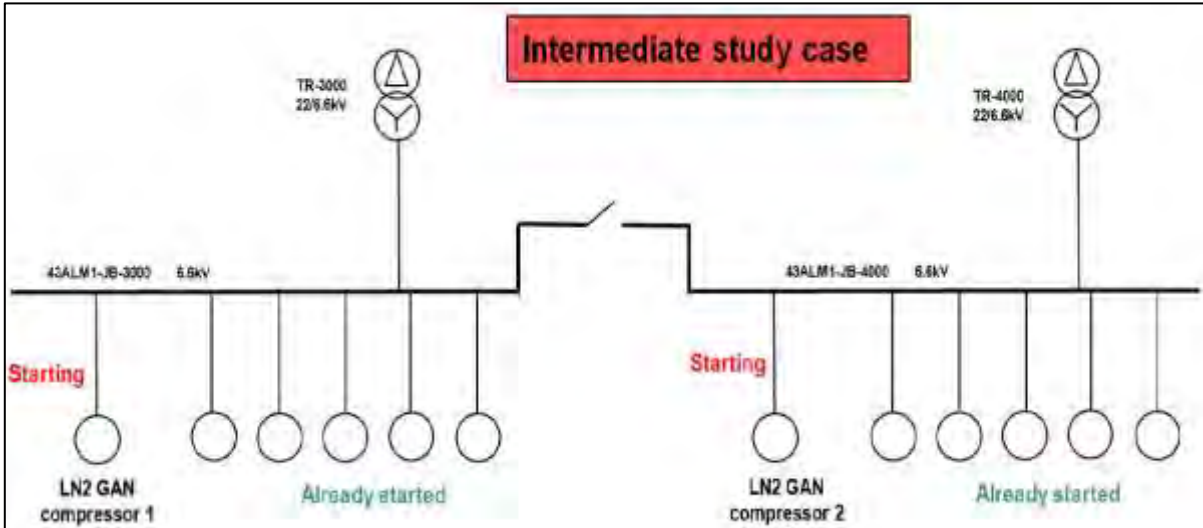


Fig. 4.7 Intermediate Study Case Configuration

c) Unfavourable Study Case

It is considered that LN GAN motor is the second one to be started (the other LN2 GAN compressor is already started) and one 22/6.6kV transformer is out of service. The busbars are coupled and the capacitor banks are not connected.

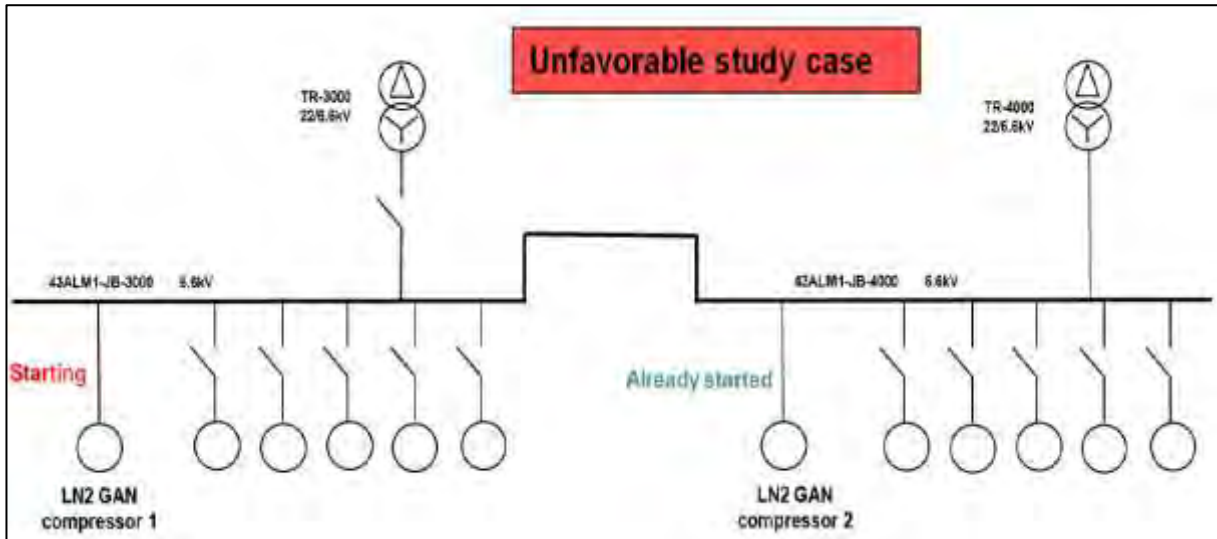


Fig. 4.8 Unfavourable Study Case Configuration

d) Most Unfavourable Study Case

The LN2 GAN motor is the last one to be started after that all the other MV motors are already at steady state and only one of the two 22/6.6 kV transformers is on service. The busbars are coupled and the capacitors banks are all connected.

Consider that the probability to have this last scenario during the starting process is very low, but it is analyzed in order to see the worst effects on the voltage.

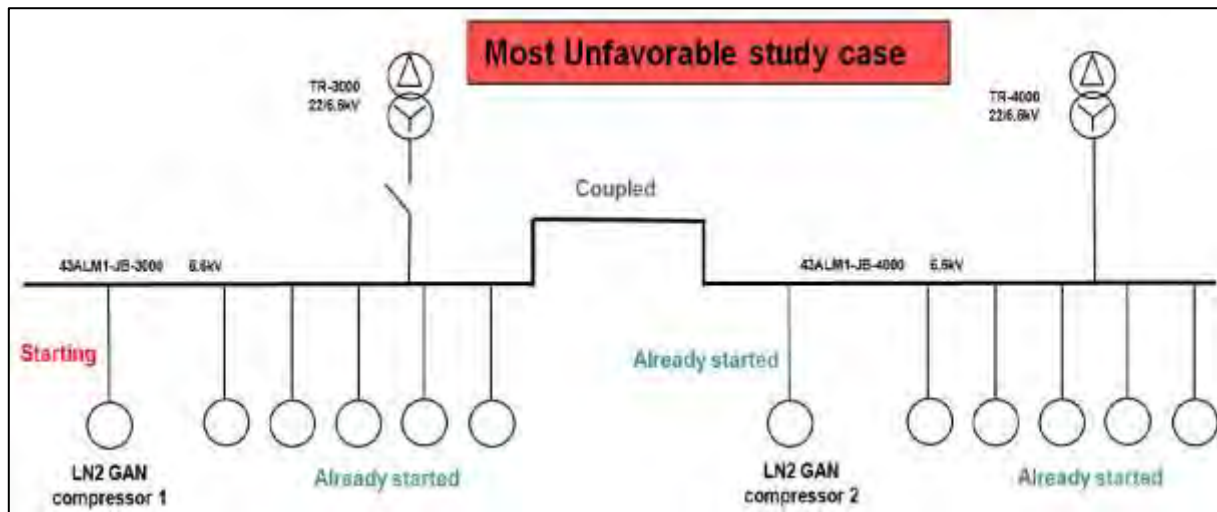


Fig. 4.9 Most Unfavourable Study Case Configuration

4.3 Analysis and Results with ETAP

For each scenario described are shown the following results, obtained using ETAP:

- The speed of the LN2 GAN motor which is set to start with the soft starter, in order to evaluate the time needed by the machine to complete the process;
- The voltage on the motor terminal bus and on busbar 43ALM1-JB-3000, so it is possible to see the impact of the starting process on the voltage and therefore to understand if the mentioned criteria are respected or not. Consider that between the motor and busbar JB-3000 there is a 100 meters cable.

To show these results within ETAP it is necessary to perform the simulations with two different modules available in the software:

- The *Motor Starting Analysis (MSA)*, that allows to determine if a motor can be started and how much time is needed to reach the rated speed, as well as to evaluate the effects on the voltage in an electrical system. This analysis is used to see the motor speed curve and not the voltage, since this module shows some inaccuracy regarding this aspect that has still to be solved;
- The *Transient Stability Analysis (TSA)*, which is designed to investigate the system dynamic responses and limits after some change or disturbance in the electrical equivalent model created [24]. It allows the reproduction of many events, such as short-circuits, opening and closing of circuit breakers and also the starting (or stopping) process of motors. In the following study this

module is used to report the voltage curves: it seems that the electrical and load models are considered more accurately and this gives better results than the ones obtainable with the MSA.

The LN2 GAN motor is coupled with a soft starter, whose settings are the following:

Starting Voltage [%]	60
TOR [seconds]	30
Current Limit [%]	295

Tab. 4.2

Before choosing these values several other combinations have been tried. The reasons for these settings are also due to the details in the datasheet and to requirements from the system:

- The voltage is set at 60% because with a lower value the motor has some trouble to start and the whole process takes more time: this aspect is linked to the big inertia of the motor-load complex (249 kg·m²). Moreover, even if a greater value is set, ETAP does not use it as the start voltage: in Fig. 4.10 it is set at 80% and it is taken into account for just an instant. This is due to the selection of the current limit, because keeping the current at a low constant value affects the natural progression of the voltage: in fact, it remains at a constant level related to the current limit selected;
- The time of the ramp is 30 seconds because in this way all the starting period is covered, bringing benefits to the voltage during the process;
- The 295% of current limit is provided by the datasheet of the soft starter and represents a big reduction considering that the starting current is 515% of the rated one without the soft starter.

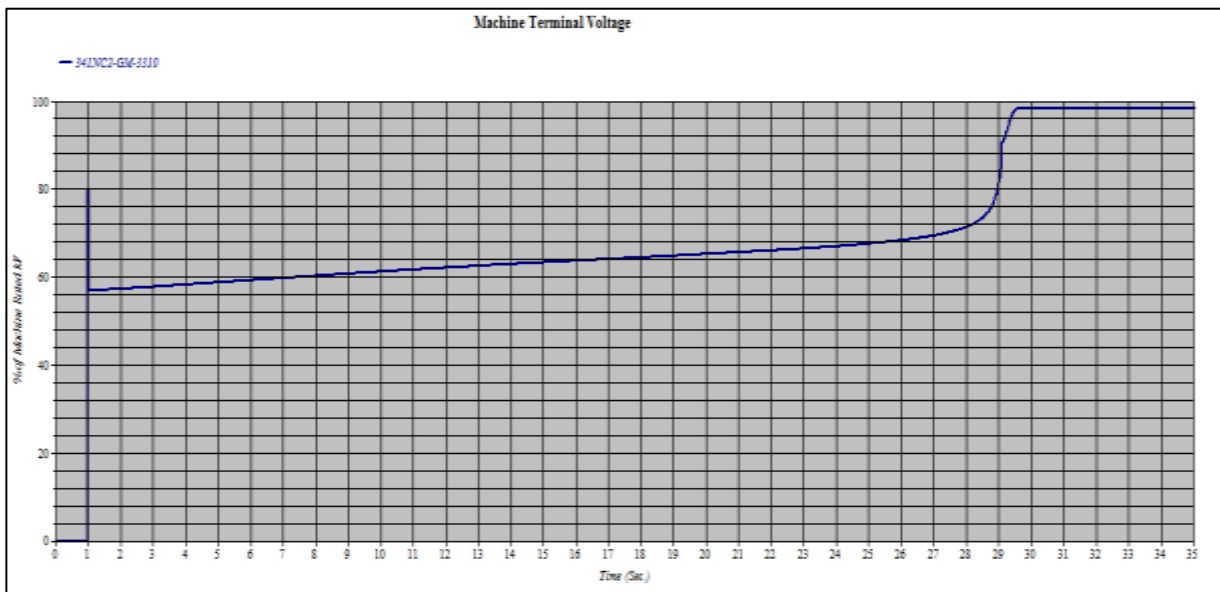


Fig. 4.10 Voltage ramp progression limited by the current limit option set

4.3.1 Normal Study Case

The speed progression is represented in Fig. 4.11: it is clear that the soft starter has an impact on the process since the motor needs almost 30 seconds to start instead of 11, as shown in Fig. 4.5 and Tab.4.1.

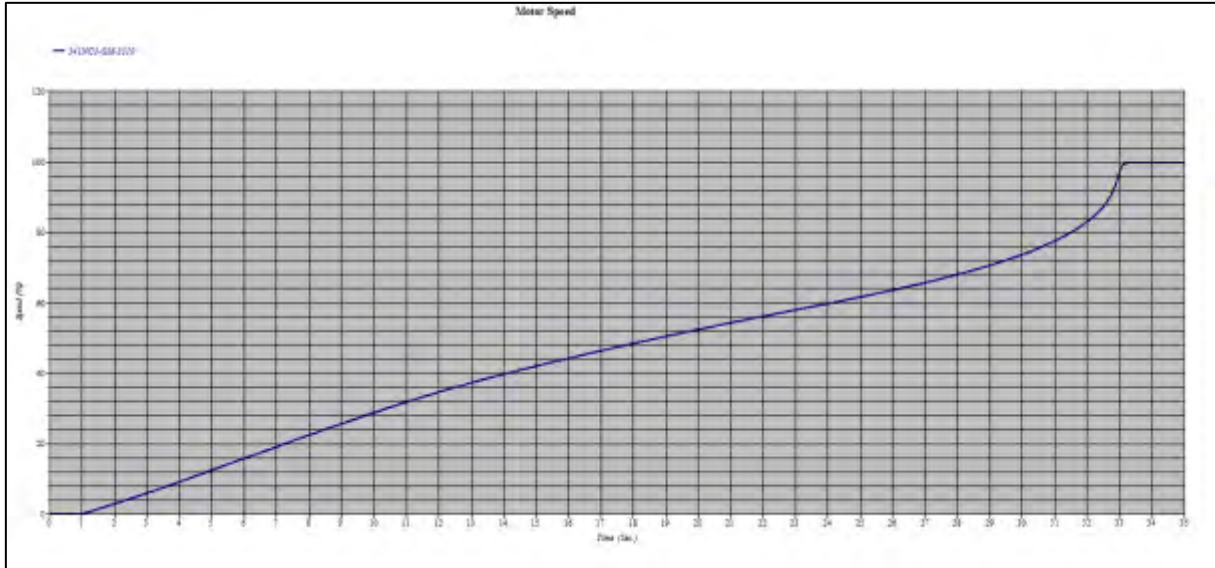


Fig. 4.11 Motor Speed with Normal Scenario

The impact on the voltage at the motor terminal and at busbar JB-3000 is the following:

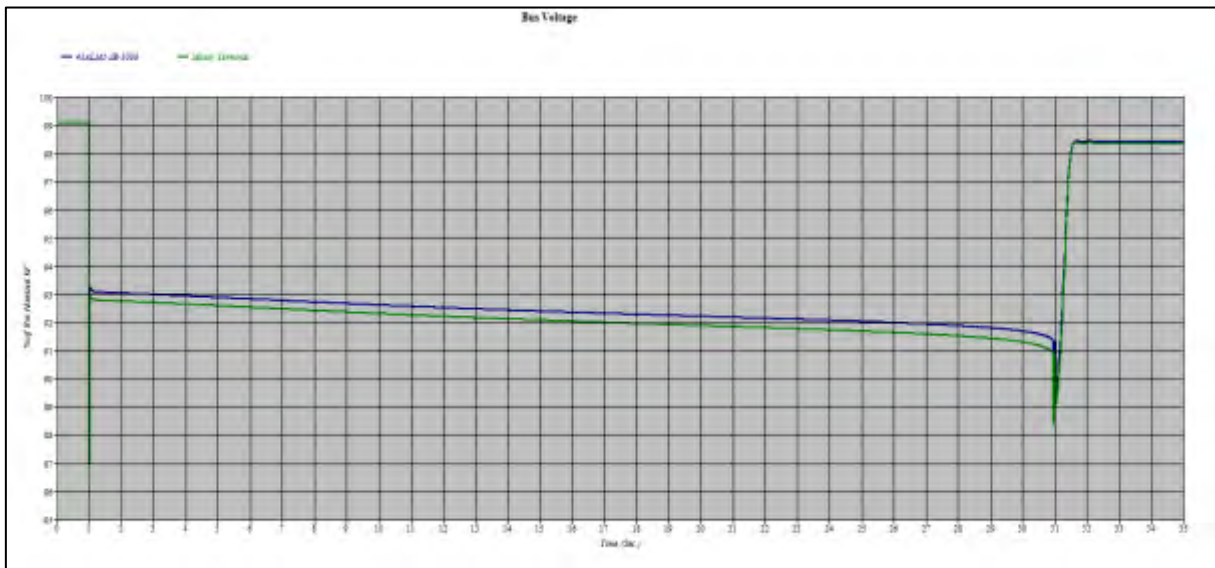


Fig. 4.12 Voltage Drop with Normal Scenario

Location	Voltage BEFORE Starting [%]	Voltage DURING Starting [%]	Voltage AFTER Starting [%]	Duration [s]
43ALM1-JB-3000	99.07	93.06	98.4	30.6

Motor Terminal	99.07	92.78	98.34	30.6
----------------	-------	-------	-------	------

Tab. 4.3

From Tab. 4.3 we can conclude that

- a) The voltage at the beginning is the same in the two points considered;
- b) After that the motor starts and at the end the voltage has a little difference in the two busses;
- c) Before completing the process, there is a quick reduction on the voltage ($t = 31$ seconds) caused by the big inertia of the motor;
- d) The voltage drop at JB-3000 is almost 6%, so the limit is respected.

4.3.2 Intermediate Study Case

The results for this scenario are the following:

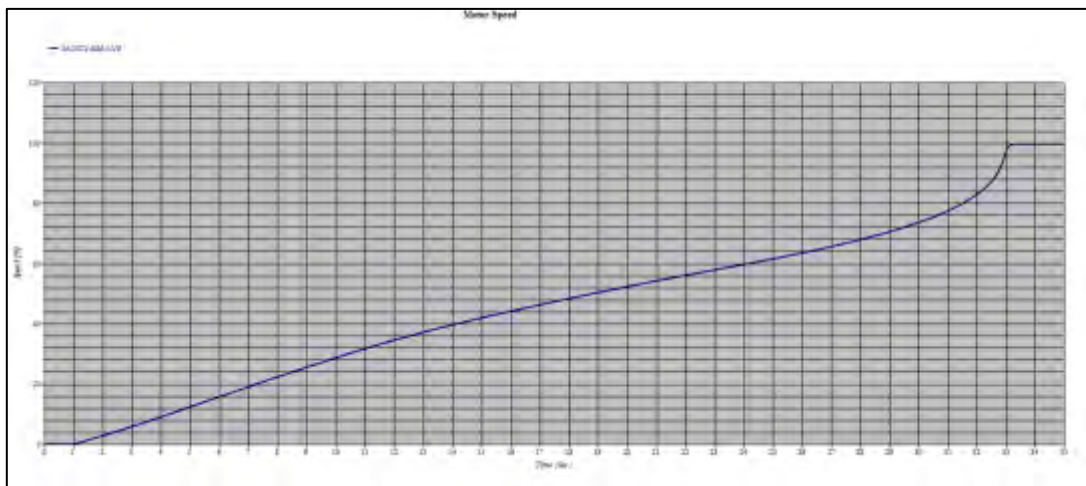


Fig. 4.13 Motor Speed with Intermediate Scenario

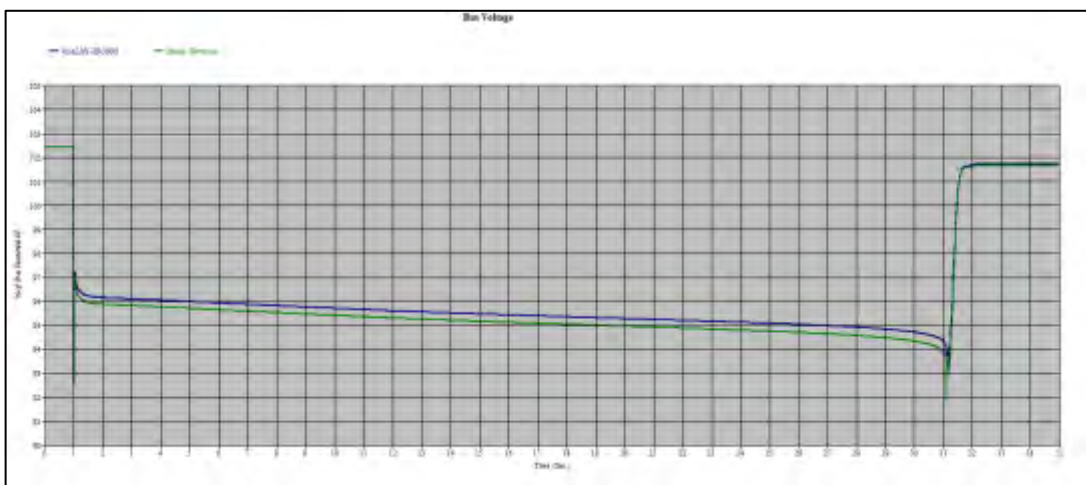


Fig. 4.14 Voltage Drop with Intermediate Scenario

Location	Voltage BEFORE Starting [%]	Voltage DURING Starting [%]	Voltage AFTER Starting [%]	Duration [s]
43ALM1-JB-3000	102.43	96.3	101.72	30.7
Motor Terminal	102.43	95.5	101.63	30.7

Tab. 4.4

Like for the Normal Study Case, points a), b) and c) are present. The voltage drop at busbar JB-3000 is respected again even if the starting configuration is less favorable for the system.

4.3.3 Unfavourable Study Case

The speed and the voltage drops are the following:

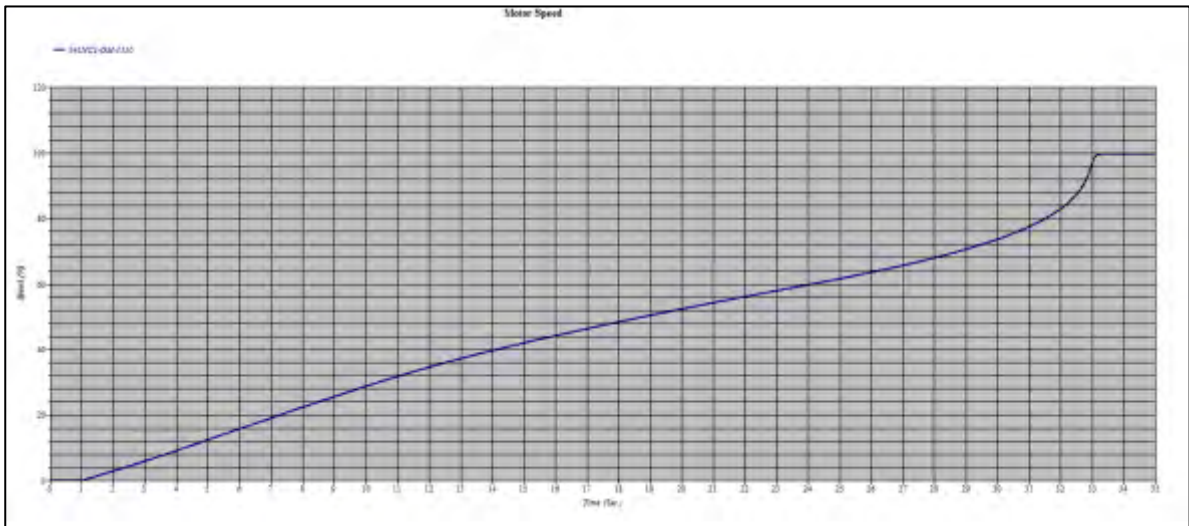


Fig. 4.15 Motor Speed with Unfavorable Scenario

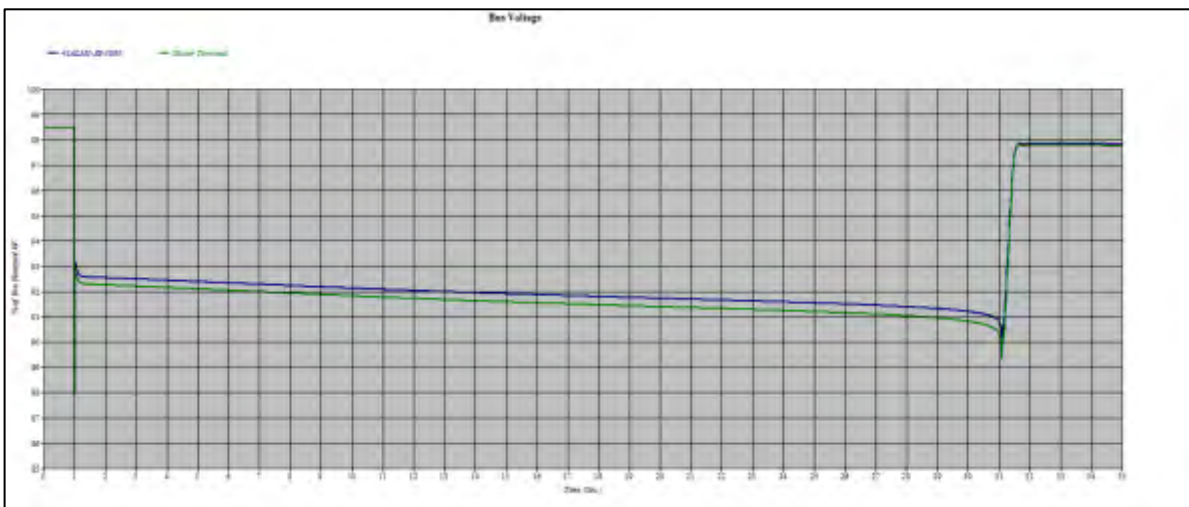


Fig. 4.16 Voltage Drop with Unfavorable Scenario

Location	Voltage BEFORE Starting [%]	Voltage DURING Starting [%]	Voltage AFTER Starting [%]	Duration [s]
43ALM1-JB-3000	98.46	92.5	97.83	30.4
Motor Terminal	98.46	92.3	97.75	30.4

Tab. 4.5

Even in this configuration points a), b) and c) are present and the voltage drop at busbar JB-3000 is respected.

4.3.4 Most Unfavourable Study Case

The results for this scenario are shown in the following images.

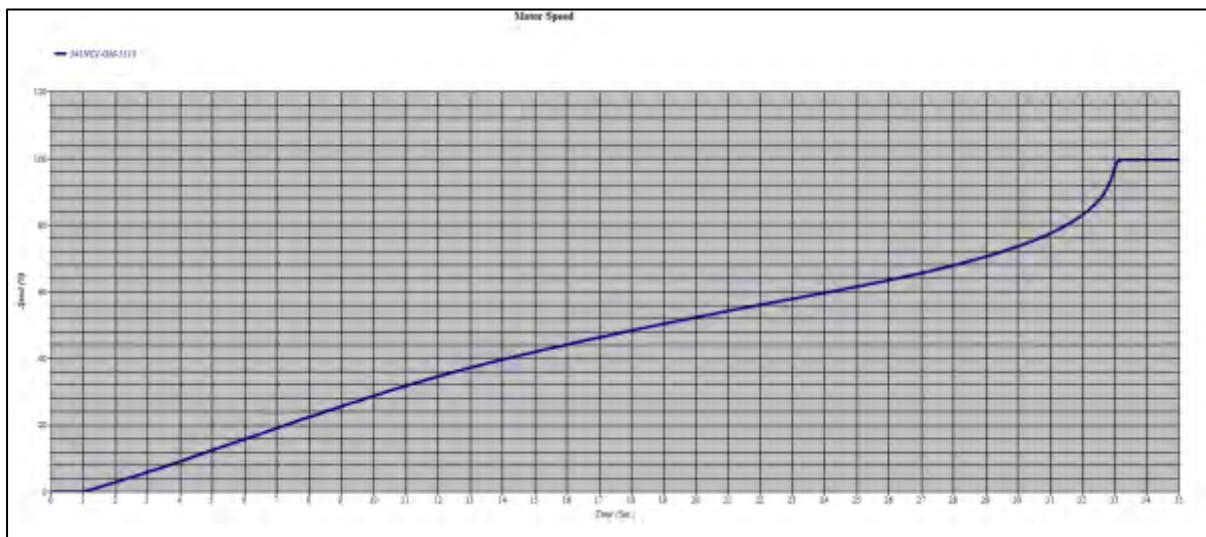


Fig. 4.17 Motor Speed with Most Unfavorable Scenario

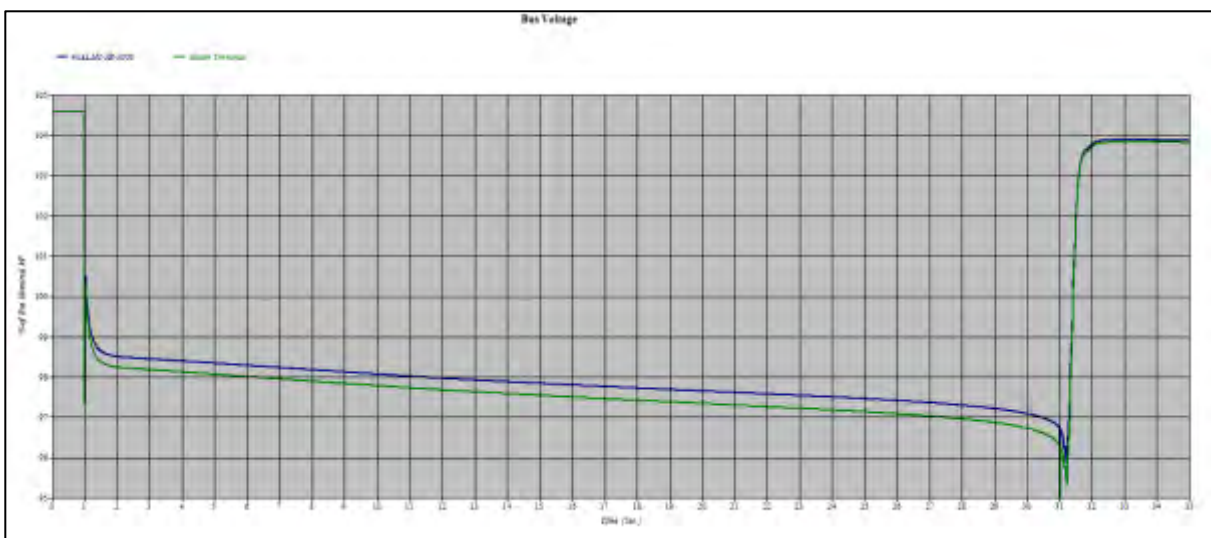


Fig. 4.18 Voltage Drop with Most Unfavorable Scenario

Location	Voltage BEFORE Starting [%]	Voltage DURING Starting [%]	Voltage AFTER Starting [%]	Duration [s]
43ALM1-JB-3000	104.6	98.5	103.87	30.5
Motor Terminal	104.6	98.2	103.79	30.5

Tab. 4.6

In the worst scenario points a), b) and c) are present again and moreover the voltage limit of 8% is not exceeded.

In conclusion, all the results obtained with ETAP show that the limits regarding the voltage drop (<8%) on MV-01 busbars and the minimum startup voltage authorized (<15%) are respected: this means that the soft starter is useful for the system as it is set, since it allows to reduce the electrical and mechanical stresses due to the starting process of such a large motor like LN2 GAN.

4.4 Analysis with SimPowerSys

A starting motor study has been done using SimPowerSys, but not with the aim of repeating the same identical simulations made with ETAP: since it is the first time at ITER that this type of analysis has been conducted in Simulink, the main goal is to start comparing some result obtained with the two programs, in order to have the possibility to do a crosscheck and to be able to evaluate in a more detailed way the systems taken into exam in the future. So the analyses studied are different from the ones shown before with ETAP.

Consequently, the Simulink model created has some simplification:

- Not the entire ITER Electrical Network is reported in the scheme, just the single branch to the 4.7 MW motor;
- Only busbar JB-3000 is included, but not JB-4000;
- Only LN2 GAN motor is in the scheme, the other MV motors are not included.

Before going into the details of the simulations done, it is appropriate to describe the SimPowerSys model built. In the equivalent model of Fig. 4.19 there are several elements, a part of them has already been described in Chapter 3 (such as the 22/6.6 kV transformer and the LN2 GAN motor), but other blocks are included because they are important to reproduce the system in the best way. Note that in Fig. 3.1, taken from the ETAP model, only MV-01 busbars are shown, but obviously in the entire electrical scheme there are other elements such as the supply electrical grid, the 400/22 kV transformers and all the busbars included in the SSEN.

The main elements of the single branch model in SimPowerSys are the following:

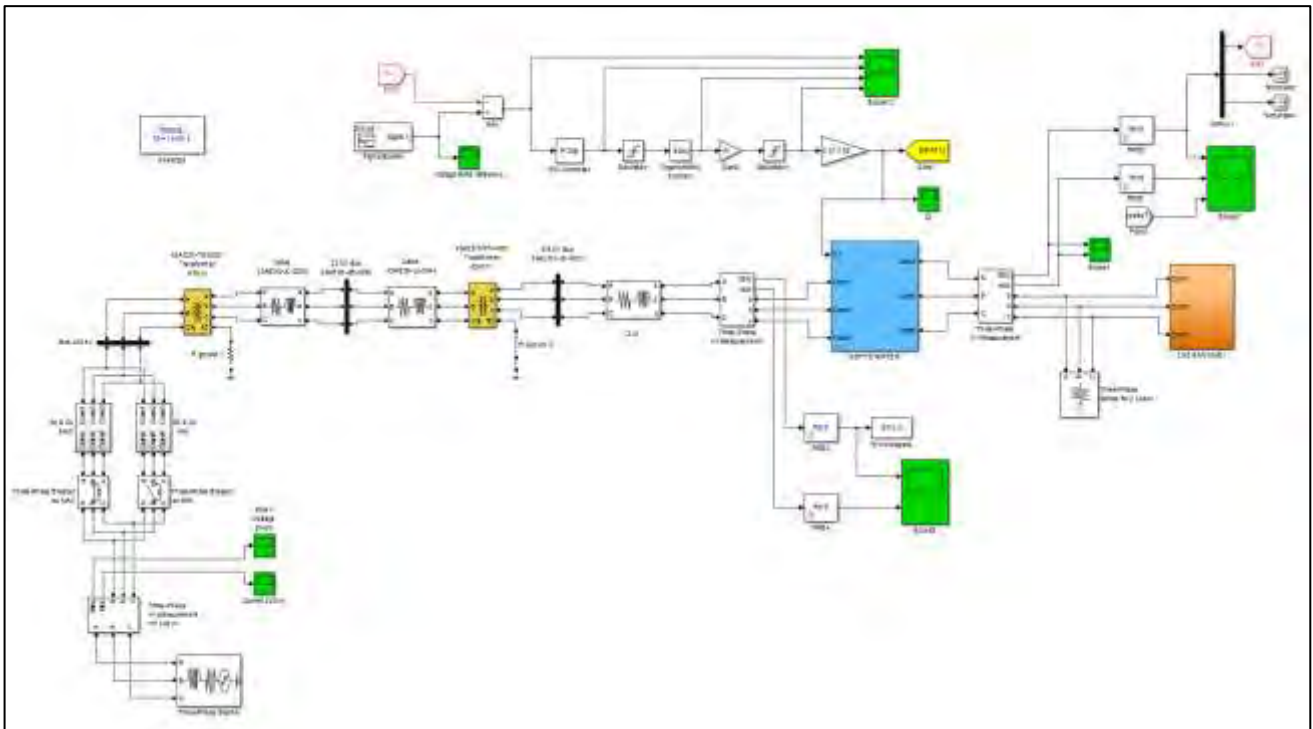


Fig. 4.19 Single Branch Equivalent Model

- The supply grid is represented with the *Three-Phase Source* block; the phases have a Y connection with an internal grounded neutral, the rated voltage used is 400 kV and the short-circuit power is set at 30 GVA (this value is justify in Chapter 5);
- Following the ETAP model construction, after the *Three-Phase Source* there is a combination of impedances useful to represent the maximum and minimum configuration for the short-circuit currents at the ITER 400 kV Substation and the values are provided by RTE;
- Transformers 400/22 kV and 22/6.6 kV are included in the scheme and the data used as input are those reported in Tab. 4.7:

Transformer	Voltage [kV]	Power [MVA]	R_1, R_2 [p.u]	L_1, L_2 [p.u]
43AC00-TS-2000	400/22	75	0.002655	0.0849
43AEM1-TR-4000	22/6.6	35	0.00183	0.05497

Tab. 4.7

- The model includes also some cable, such as 43AE00-JL-2000 and JL-0044, represented with the *Three-Phase series RLC Branch* block, selecting only the combination RL;
- Both the LN2 GAN motor and the soft starter are built inside a subsystem and they require a deeper description since they are the core of the model.

4.4.1 LN2 GAN Motor in SimPowerSys

The motor subsystem is shown in Fig. 4.20.

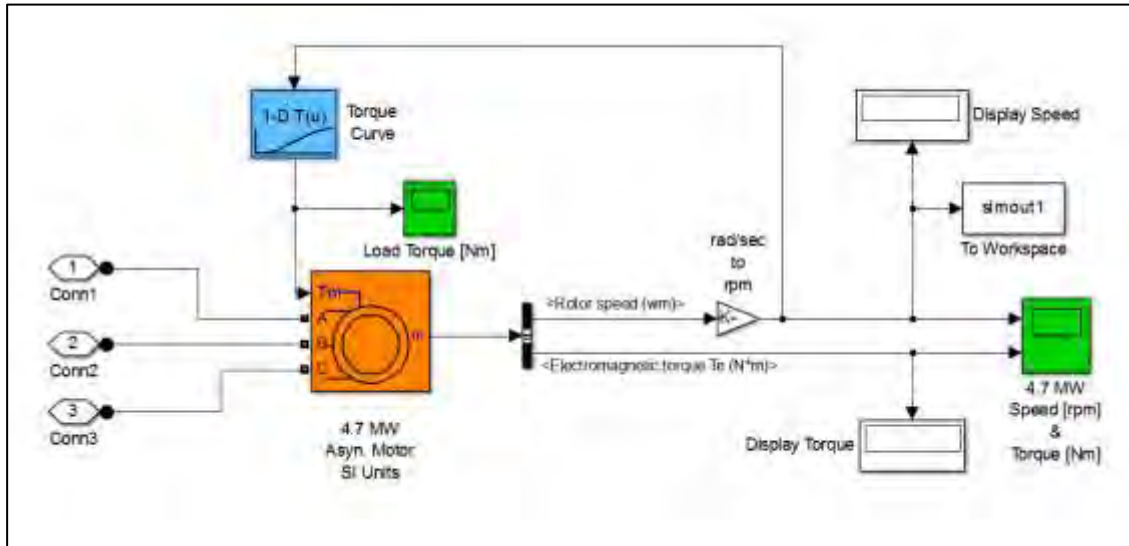


Fig. 4.20 Asynchronous Motor in Simulink

The motor used is asynchronous with a single squirrel cage, with the input data taken from Tab. 3.1-3.2 and expressed in the SI units following formulas [2.2] [2.3]. Since this analysis is dedicated to the starting process, under the entry field *Initial Conditions*, inside the motor block, are used the following parameters:

Slip	Electrical Angle [°]	Stator Current Magnitude [A]	Stator Current Phase [°]
1.0	0	0	0

Tab. 4.8

The output signals measured are the electromagnetic torque (Nm) and the speed (rpm): both are shown in order to verify if the machine is acting like a motor during the simulation and to have an idea of the starting process as well. The speed is also used as input in a *Lookup Table* used to create the correct torque-speed characteristic of the load connected to the motor: the values of the torque are taken from Tab. 3.3, but expressed in Nm and not in percentage.

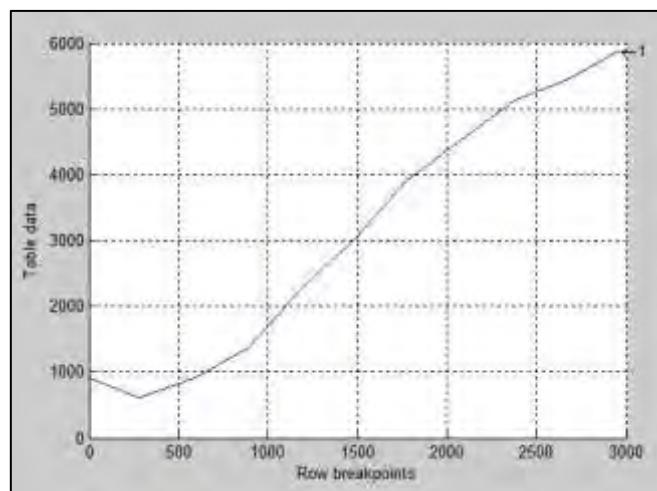


Fig. 4.21 Lookup Table Output

4.4.2 Soft Starter in SimPowerSys

The model created is a draft, i.e. it is a starting point to be used for preliminary analyses, such as this one, and therefore it needs to be improved and upgraded. Not many details about the soft starter are available: this aspect is positive and negative at the same time, because it allows a custom made control to be created, but on the other hand there is no precise indication if it is correct or not.

The final goal is to reproduce a voltage in output from the soft starter similar to the ramp shown in Fig. 4.4: in achieving this, for each phase two thyristors are connected in an antiparallel configuration, so one will conduct during the positive semi-wave and the other during the negative semi-wave.

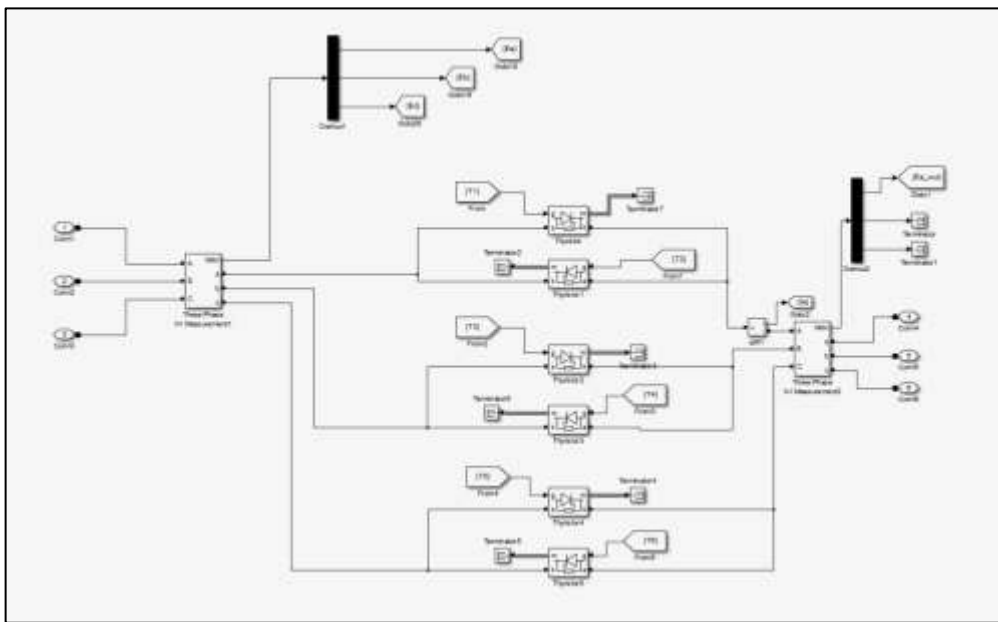


Fig. 4.22 Disposition of the thyristors

The phase-to-ground voltage of each phase is measured and sent to the loop of Fig. 4.23 and the signal useful to control these thyristors is generated in the following way:

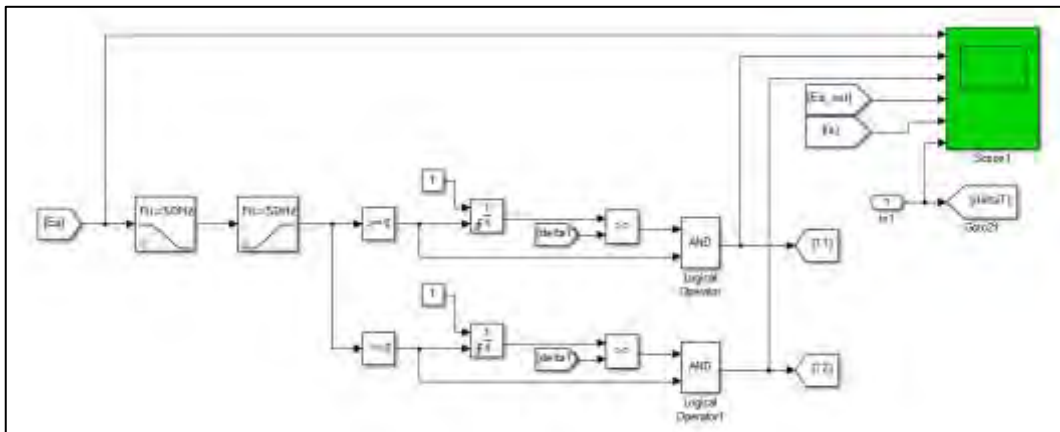


Fig. 4.23 Phase a Control

- a) At first, the voltage goes through a low-pass and high-pass filter in order to obtain and use only a wave closer to the fundamental as reference;
- b) Two *Compare to Zero* blocks allow to divide the filtered signal: whenever it is positive it will pass only through the upper block, vice versa when it is negative through the lower one. In this way it is possible to distinguish the signals to control the two thyristors in antiparallel;
- c) When the output signal from the *Compare to Zero* block is not zero, an *Integrator* block will integrate a constant equal to 1 in order to generate a ramp of time ($\int 1 dt = t$), which goes from zero to 0.01 (i.e. half of the period with 50 Hz as frequency);
- d) This ramp is then compared through a *Relational Operator* block with “deltaT”, i.e. the required delay expressed as a time and not as an angle: when the first input (the ramp) is greater than or equal to the second one (deltaT) then the block will generate a signal. In this way it is possible to determine the conduction time of each thyristor during the appropriate semi-period (0-0.01 seconds): until “deltaT” is greater than the ramp the thyristor will not be able to conduct, after that the delay is inferior it will start to operate. This reasoning is described in Fig. 4.24 where it is used a “deltaT” equal to 0.004 seconds: the conduction will start at 0.004 and will continue until 0.01 seconds.

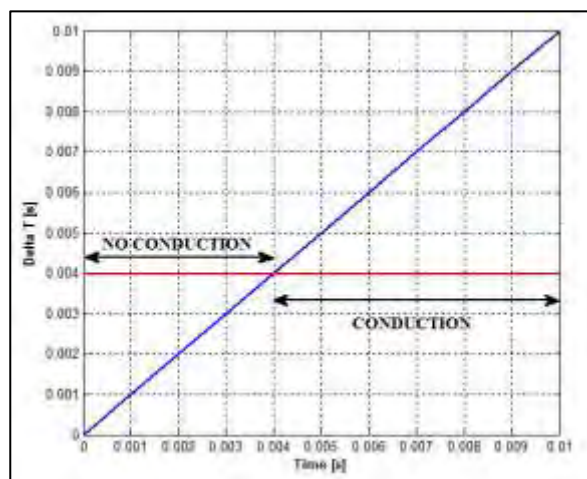


Fig. 4.24 Conduction Period

- e) The result is then sent to a *Logical Operator* (applying the “AND” function) together with the signal in output from the *Compare to Zero* block: this is just a precaution to be sure that the control is generated during the correct portion of semi-period.

The delay “deltaT” introduced in point “d” is created in this way (see Fig. 4.25):

- f) The phase-to-ground voltage measured at the motor terminal is compared with a reference signal generated by a *Signal Builder* block (Fig. 4.26): the reference taken is a ramp and is fundamental for managing the delay;
- g) The difference between the two signals is sent to a PI regulator ($P = 0.00005$, $I = 0.001$);
- h) The output from the regulator is then limited between +1 and -1 by a *Saturation* block;

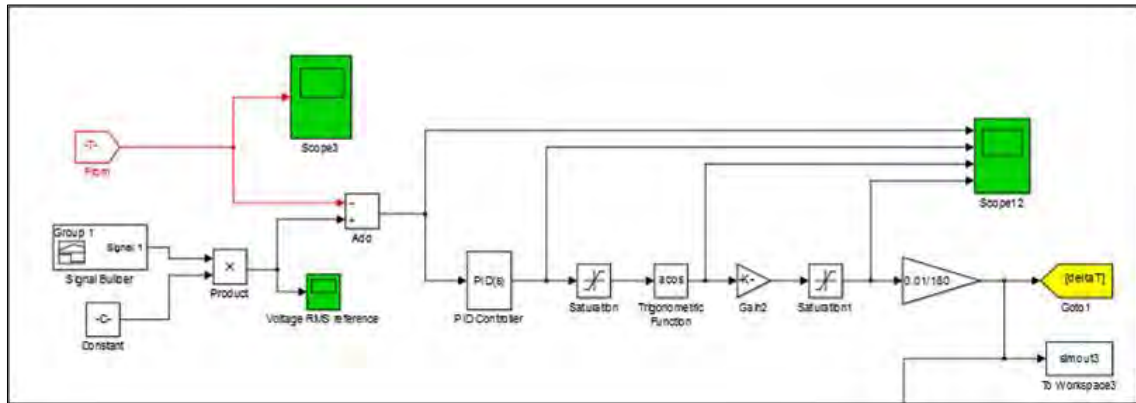


Fig. 4.25 Loop to Generate the Delay

- i) The signal is then applied to a trigonometric function (*arccosine* in this case) in order to convert it into an angle. This angle is expressed in radians and so is multiplied by $180/\pi$ to get degrees as unit;
- j) The result, i.e. the alpha delay, is limited between 0° and 180° , since it can only be a positive value;
- k) To express the delay in seconds, it is sufficient to multiply it per $0.01/180$.

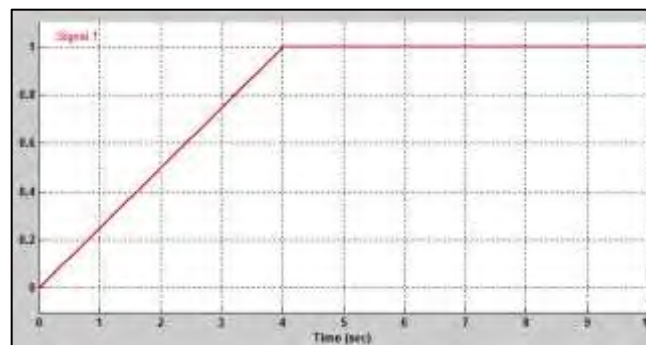


Fig. 4.26 Signal Builder Output

What is not included in the described control is the current limit: this option is available in ETAP and allows the reduction of the voltage drops during the starting process. In order to have a reasonable comparison between the two programs, the current limit option in ETAP is not considered: note that in this way big voltage drops are expected. Obviously, the ETAP model used is simpler in its construction with just one branch and only the LN2 GAN motor for the simulations.

4.5 Comparison and Results

As explained in Chapter 2, there are differences between ETAP and SimPowerSys in the parameters needed to describe the electrical motor:

- in ETAP there is the distinction between the impedance with the locked rotor (LR) and full load (FL) conditions (see Tab. 2.1), in SimPowerSys instead there is only the possibility to insert the value of

resistance and reactance characteristic of the stator and rotor windings inside the motor, so there is no way to distinguish the impedance in LR and FL scenarios;

- In ETAP there are numerous data to fill, such as breakdown torque, locked rotor current, power factor and efficiency in many different load condition (100%, 75%, 50% of the load), while in SimPowerSys the required data are less, only some information regarding the power, the voltage, the impedance and the inertia.

These aspects bring differences in the results, so the two programs are unlikely to give the same identical output. To start comparing the two softwares, it is better to evaluate the differences in the motor starting with the DOL technique and then introduce the soft starter in the process.

4.5.1 Differences with DOL Technique

In the first DOL starting comparison made, the distinction between the LR and FL impedance in ETAP is retained, so the values used are the following:

ETAP	
R_s [p.u]	0.0137
X_s [p.u]	0.0955
$R_{r\text{lr}}$ [p.u]	0.0212
$R_{r\text{fl}}$ [p.u]	0.0112
$X_{r\text{lr}}$ [p.u]	0.0955
$X_{r\text{fl}}$ [p.u]	0.1435
X_m [p.u]	6.38

Tab. 4.8

SimPowerSys	
R_s [Ohm]	0.109
L_s [mH]	2.42
R_r [Ohm]	0.1687
L_r [mH]	2.42
L_m [H]	0.16174

Tab. 4.9

The results with the values of Tab. 4.8 and 4.9 are the following:

Program	Δt [s]	V_{min} [%]	I_{max} [%]
ETAP	13.1	84.9	440
SimPowerSys	7.6	85.6	443

Tab. 4.10

The starting time is not the same, 13.1 seconds versus 7.6, and this is caused by the distinction in ETAP between LR and FL: in fact, with different values the torque produced by the motor is lower during the entire starting

process and therefore it takes more time to complete it; instead using the same impedance in LR and FL conditions the electromagnetic torque is higher and the process is faster, as actually happens in Simulink. Essentially the motor is not the same and so the characteristic is different in the two cases.

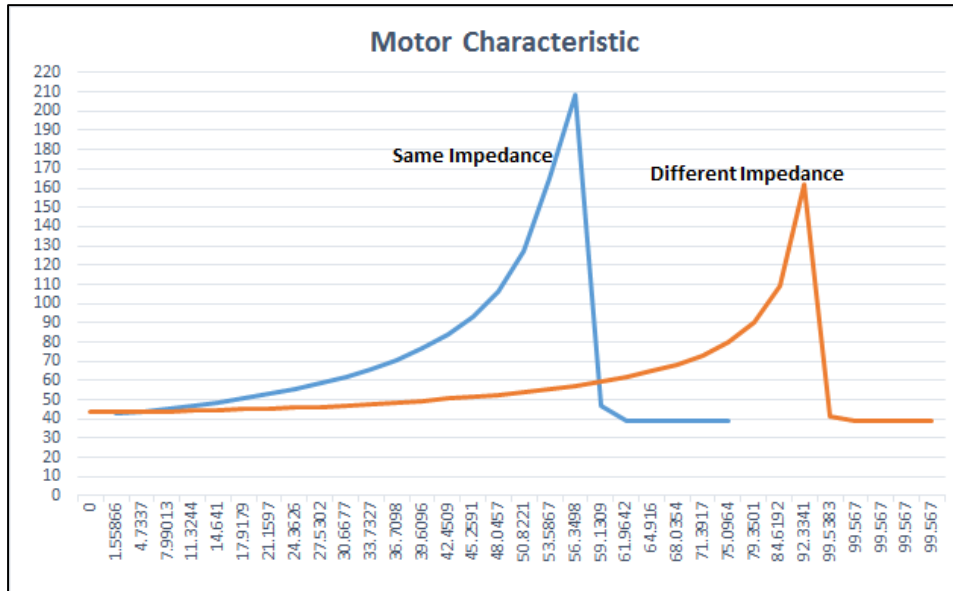


Fig. 4.27 Different Torque-Speed Characteristic

If the same simulation with DOL is repeated using the same values in LR and FL, then the results will be similar:

ETAP	
R_s [p.u]	0.0137
X_s [p.u]	0.0955
R_{rlr} [p.u]	0.0212
R_{rn} [p.u]	0.0212
X_{rlr} [p.u]	0.0955
X_{rn} [p.u]	0.0955
X_m [p.u]	6.38

Tab. 4.11

Program	Δt [s]	V_{min} [%]	I_{max} [%]
ETAP	8.5	85.9	440
SimPowerSys	7.6	85.6	443

Tab. 4.12

Now the starting times are closer and moreover the voltage drop along with the maximum current reached during the process are almost the same for both the software.

In conclusion, the DOL technique for the LN2 GAN motor gives an identical result when the same values of resistance and reactance for LR and FL are used in ETAP.

4.5.2 Differences Using the Soft Starter

The right way to compare the two softwares is using the same identical settings in both and to do this it is necessary to recreate the same voltage ramp through the soft starter and without including the current limit option in ETAP.

In order to have a better overview of the possible differences, three ramps are simulated and the settings used are the following:

- Time of the ramp equal to 20, 30 and 40 seconds respectively;
- Initial voltage set at 60% of the rated one;
- Finale voltage at 100%.

With these settings ETAP gives the results shown in Tab. 4.14:

TOR [s]	Starting Time [s]	V _{min} [%]	I _{max} [%]
20	12	88.23	391
30	14	89.7	367
40	16	90.4	353

Tab. 4.14

On the other side, in SimPowerSys the results obtained are the following:

TOR [s]	Starting Time [s]	V _{min} [%]	I _{max} [%]
20	12	88	386
30	13.5	88	365
40	15	89	355

Tab. 4.15

In Fig. 4.28 and 4.29 are reported an example of the speed and the voltage drop curves in output from SimPowerSys in order to give a better idea of the quality of the results.

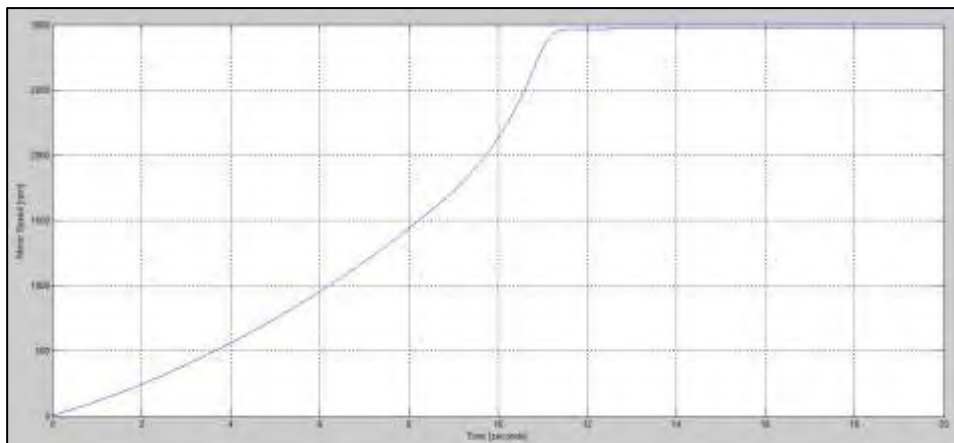


Fig. 4.28 Motor Speed with a TOR of 20 seconds

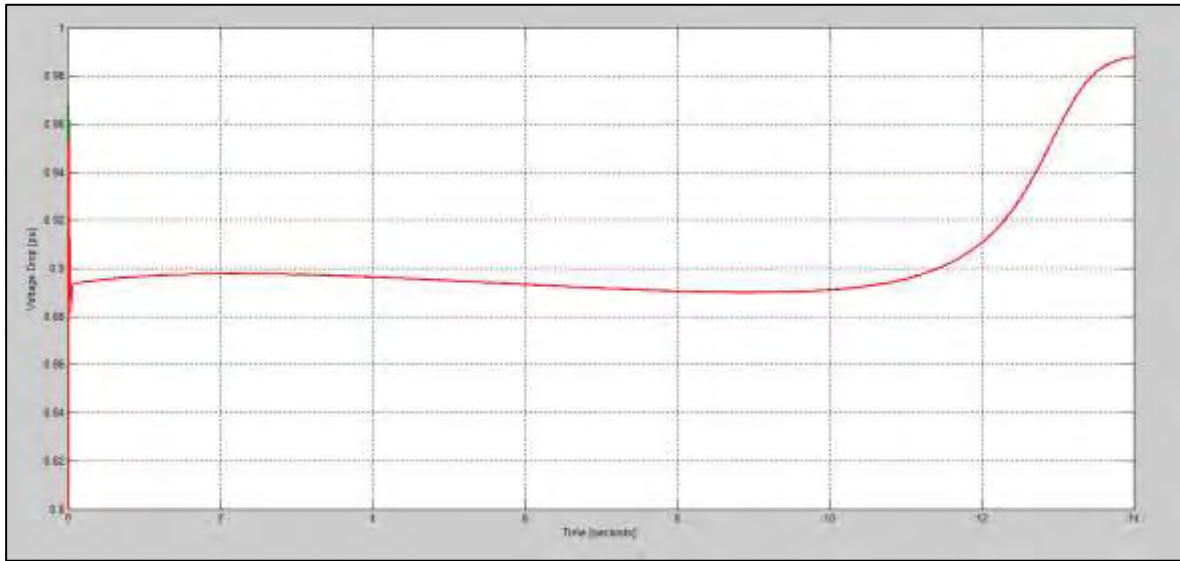


Fig. 4.29 Voltage drop with a TOR of 20 seconds

As it can be noticed from Tab. 4.14 and 4.15, the final results are very close, so proving that the Simulink model has been created correctly and moreover that ETAP is a reliable software for this type of analyses. The little differences are due to the solver used by the programs and to the data inserted into the blocks to build the schemes: as said, in ETAP there is the possibility to describe in a very detailed way all the elements, while in SimPowerSys the input parameters needed are less and therefore this aspect brings diversities.

Differences between ETAP and SimPowerSys			
TOR [s]	Starting Time [s]	V_{min} [%]	I_{max} [%]
20	0	0.23	5
30	0.5	1.7	2
40	1	1.4	2

Tab. 4.16

5. VOLTAGE REDUCTION DUE TO EXTERNAL FAULTS AND EFFECTS ON THE MV-01 MOTORS

This chapter will deal the problem of faults, both three phase and line-ground, on the external line in order to quantify the reduction of voltage at ITER Prionnet.

5.1 Faults and the Consequences on the MV Motors

One of the problems that ITER plant will have to face, when it will be in operation, is the possible presence of faults, both internal and external to the network. These faults, primarily short circuits, could cause a reduction on the voltage and the drop can be different considering the type of the fault (three phase or line-ground) and its position.

As said, in the SSEN the majority of the loads are asynchronous motors, whose operation could be affected by the voltage changes: in fact, the speed of the motors starts to decrease when the voltage is reduced, with a duration related to that of the fault, and this means that

- When the fault is solved the motors begin a new and unexpected starting process, much shorter than the programmed one, with all the problems related to the high current and high demand of power;
- The speed could go even below the accepted limit for a safe operation of the load connected and this requires a disconnection of the motor, so compromising the fusion process.

If the fault is extinguished after that the circuit breaker recloses the circuit the problem is just for hundreds of milliseconds and so not very dangerous since the inertia of the motors-load complex is not low, but if it would last longer there is the possibility that the speed will decrease over the accepted limit, bringing the motor out of service. Of course the faults cannot be foresee and prevented, but what can be studied is the magnitude of the voltage drop with all the types of short circuit faults and in different positions: in fact in this way it is possible to know which are the worst situations for the operation of the motors and, as a result, it could be found a solution to avoid to disconnect them and to keep the plant on service.

The studies made are focused only on the external faults because, since they can happen in different positions of the line, they bring diverse impacts on the voltage measured at ITER Prionnet and therefore on the speed of the motors and the fusion process: for example, a short circuit far from ITER substation could bring a lower impact on the voltage than one close to the plant.

The types of faults considered are line-ground and line-line caused by lightning strikes: after that a lightning hits a phase, or all the phases, there are waves of high voltage and current propagating over the line and consequently

the circuit breakers will open; with the breakers open for a short period of time (typically 100 milliseconds) the voltage will be equal to zero in the strike point.

The aims of the analysis are, as first, to evaluate the magnitude of the voltage reduction at ITER Prionnet caused by faults applied in various points of the grid and secondly to verify the effects on the motors connected to the 43ALM1-JB-3000 and 4000 busbars: in undertaking the study, an equivalent SimpowerSys model of the external grid and a scheme of the internal network of the plant were created.

For this study several assumptions have been made due to the lack of precise information about the lines, the electrical grid, the loads connected to the busbars and moreover because some data are not the definitive ones: this is a preliminary work useful to start to understand the impact of some of the problems originating from the external grid and later when ITER will be in possession of more information regarding the various elements the model has to be updated.

5.2 External Electrical Grid

As said before, ITER will be connected to the French 400 kV transmission network operated by RTE and this grid has many branches.

What will be described are the lines, the elements directly connected to ITER, and not all the electrical systems, since the following analysis will be focused on faults applied on one of these lines.

In Fig. 5.1 it is shown an equivalent model of the external grid.

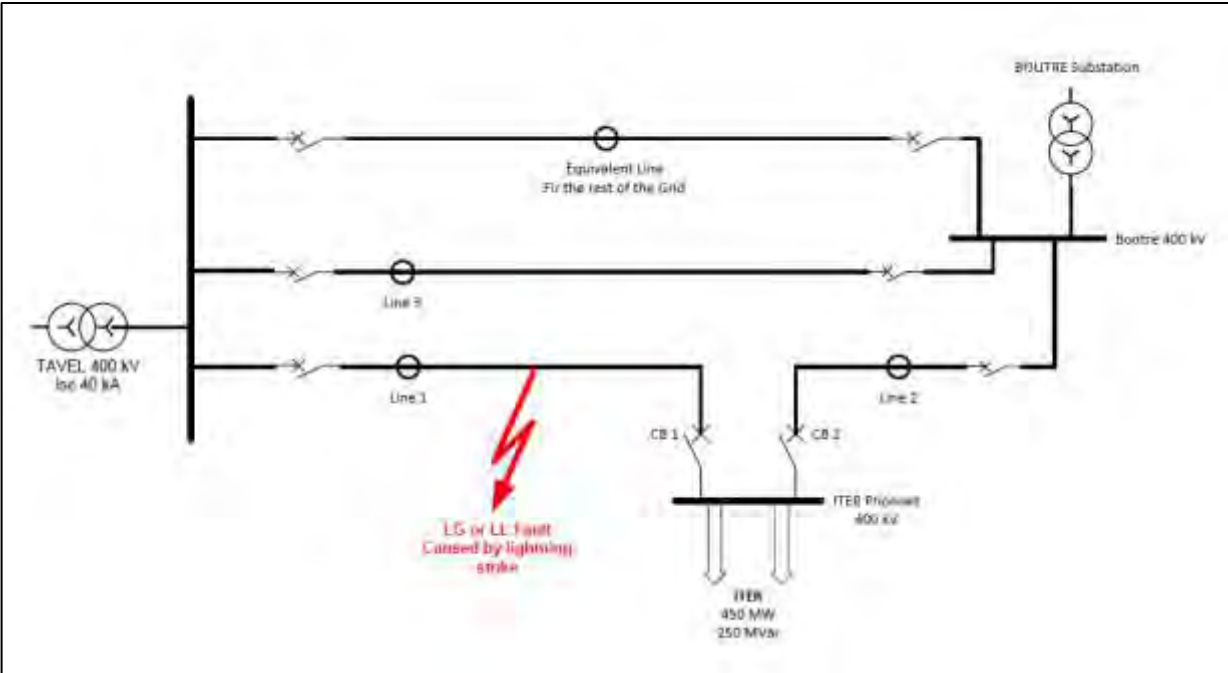


Fig. 5.1 Equivalent scheme of the external grid

ITER Prionnet is the 400 kV substation, erected and completed by French grid operator in 2012, which will provide the required power to supply ITER electrical demand and will be connected to the 400 kV grid by a double line circuit.

The main power will arrive from two substations:

- Tavel, 400 kV, located to the west of Avignon;
- Boutre, 220 kV, 6 km south-east of ITER platform.

From Tavel two lines will depart in the direction of ITER, both around 120-130 km: one (Line 1) will be directly connected to ITER Prionnet and the other (Line 3) to Boutre Substation.

From Boutre Substation will depart another branch (Line 2) of almost 10 km directed to Prionnet. The length of the two branches entering in Prionnet already takes into account the distance between the end of the lines and the connections to the substation.

The 400 kV "Boutre-Tavel" power line is an essential link in the interconnected European grid, it supplies electricity to a vast area of south-eastern France and, since the construction of a derivation in the late 1980s, also to the CEA-Euratom tokamak Tore Supra [25].

The anticipated needs of ITER have led to an extension and a reinforcement of the Tore Supra derivation and the new power highway delivers 400 kV by way of two power lines.

This connection is planned in this way in order to maintain power to ITER plant: if, for example, there are problems on the lines from Tavel then the plant will be connected to Boutre and vice versa.

These two substations, as well as the lines derived from them, are part of the south French electrical grid and this is why in the scheme of Fig. 5.1 there is also an equivalent line representing the rest of the system: in Provence there are several power plants, such as thermal nuclear and hydro, and therefore the 400 or 220 kV substations are very diffused, as in part shown in Fig. 5.2.



Fig. 5.2 RTE panoramic

5.2.1 Known Data and Assumptions

This analysis includes available information about the external lines, the HV substations, ITER intended as a unique load, but currently not all details are available or definitive: in fact RTE does not share a lot of data about the grid and it is not easy to reproduce an equivalent model of it. Moreover, ITER will be a dynamic load since steady state and pulse state operations are foreseen: it is not simple to determine the precise power that will be required by the plant and to report it in the simulations.

Consequently several hypotheses have been made in order to recreate a model and to do the simulations.

In the first instance, it is better to start from the known data.

a) Electrical Lines

RTE has furnished a document with information about Line 1 and Line 2 (referring to Fig. 5.1), the short circuit currents at ITER Prionnet and also some criteria to respect, such as the elimination of a fault inside the network or the grounding system [26].

The actual details regarding Line 1 and 2 are the following:

Line	R_d [Ohm/km]	R_o [Ohm/km]	L_d [mH/km]	L_o [mH/km]	D [km]
1	0.0198	0.16682	0.84225	2.4366	125.7
2	0.0176	0.15375	0.892	2.46	9.6

Tab. 5.1

What can be noticed from Tab. 5.1 are the similar values of the two lines: this is an aspect that was taken into account to determine the input data of the rest of the electrical grid.

On the other side, note that RTE does not give the capacity to the ground (F/km) and therefore this is one of the values hypothesized for all the lines.

In the simulations the faults are applied only in different positions of Line 1, because it is longer than Line 2 and the data reported are reliable since they are given by RTE.

b) ITER Prionnet

When considering the short circuit currents at Prionnet, RTE makes the distinction between two different configurations for both line-line and line-ground fault:

- “Maximum” configuration, when both the circuit breakers CB1 and CB2 are closed, so the current is distributed between all the incoming lines;
- “Minimum” configuration, with just CB1 closed and CB2 open. In this scenario only Line 1 is connected to Prionnet.

The short circuit currents are calculated according to the IEC 60909 standard [27] and the consequent power represents the RTE grid seen from Prionnet, with the substation considered as a passive element. According to IEC 60909, the c factor applied to calculate the maximum current is 1.1.

The short circuit currents and powers are shown in the following table:

ITER Prionnet	Maximum Configuration	Minimum Configuration
I _{sc} L-L [kA]	15.9	5.6
I _{sc} L-G [kA]	13.6	4.5
SC L-L Power [GVA]	12.117	3.88
SC L-G Power [GVA]	10.364	3.117

Tab. 5.2

The power chosen to represent the ITER loads is shown in Tab. 5.3:

Active Power [MW]	Reactive Power [MVar]
450	250

Tab. 5.3

This choice consists of the both the steady state operation power (130 MW required) and an average of the pulsed power (fixed as maximum at 500 MW): the plant will have to maintain constantly a certain pulsed power and also additional heating system but not at the maximum performances, because the type of pulse foreseen will be around some hundreds of seconds and for this it is estimated that 300-350 MW should be sufficient. Therefore, an active total power of 450 MW could be a correct value for the simulations.

c) Tavel 400 kV Substation

Regarding Tavel Substation, the only known information is that the maximum short circuit current is around 40 kA and so, considering this value as the starting point, the related power and the representative impedance are the following:

- Short circuit power

$$S_{sc} = \sqrt{3} c V_n I_{sc} \quad [5.1]$$

$$S_{sc} = \sqrt{3} \cdot 1.1 \cdot 400000 \cdot 40000$$

$$S_{sc} = 30 \text{ [GVA]}$$

- Impedance

$$z_{Tavel} = \frac{c \cdot V_n / \sqrt{3}}{I_{sc}} \quad [5.2]$$

$$z_{Tavel} = \frac{1.1 \cdot 400000/\sqrt{3}}{40000}$$

$$z_{Tavel} = 6.4533 [\Omega]$$

With the hypothesis of $X/R = 10$, the resistance and the reactance can be calculated in this way:

$$z_{Tavel} = \sqrt{R^2 + X^2} = 6.4533 [\Omega] \quad [5.3]$$

$$z_{Tavel} = \sqrt{R^2 + 100 \cdot X^2}$$

$$z_{Tavel} = \sqrt{101 \cdot R^2}$$

$$R = \frac{z_{Tavel}}{\sqrt{101}} = 6.4533$$

$$R = 0.64213 [\Omega]$$

$$X = 6.4213 [\Omega]$$

Tavel Substation will have these data in the equivalent model:

R [Ohm]	X [Ohm]	I _{sc} [kA]	S _{sc} [GVA]
0.64213	6.4213	40	30

Tab. 5.4

With regard to the rest of the grid, the method used to determine the impedance of the lines is explained in the following chapter, with the help of the Simulink model created.

5.3 External Grid Equivalent Model with SimPowerSys

In Fig. 5.3 the diagram that has been implemented in Simulink.

In this scheme are clearly distinguished the elements described previously and they are modelled and adapted to Simulink in the following way:

- Tavel Substation is represented by the *Three Phase Voltage Source* block, with the short circuit power and the impedance set with the values shown in Tab. 5.4. The three sources are connected in Y to an internal grounded neutral and the nominal phase-to-phase voltage is 400 kV; note that the voltage is set to 440 kV (i.e. $c \cdot V_n$) when we want to calculate the maximum short circuit current;
- ITER is modelled with the *Three-Phase Series Load*, choosing the combination R-L (so without any C) with the neutral grounded; the block is filled with the values of Tab. 5.3;
- For Line 1 and Line 2 are used the data of Tab. 5.1, but with some change and addition:

- The value of the zero sequence inductance in Line 1 has been changed in 1.85 mH/km in order to obtain the correct line-ground short circuit current with the minimum configuration (see Tab. 5.2);

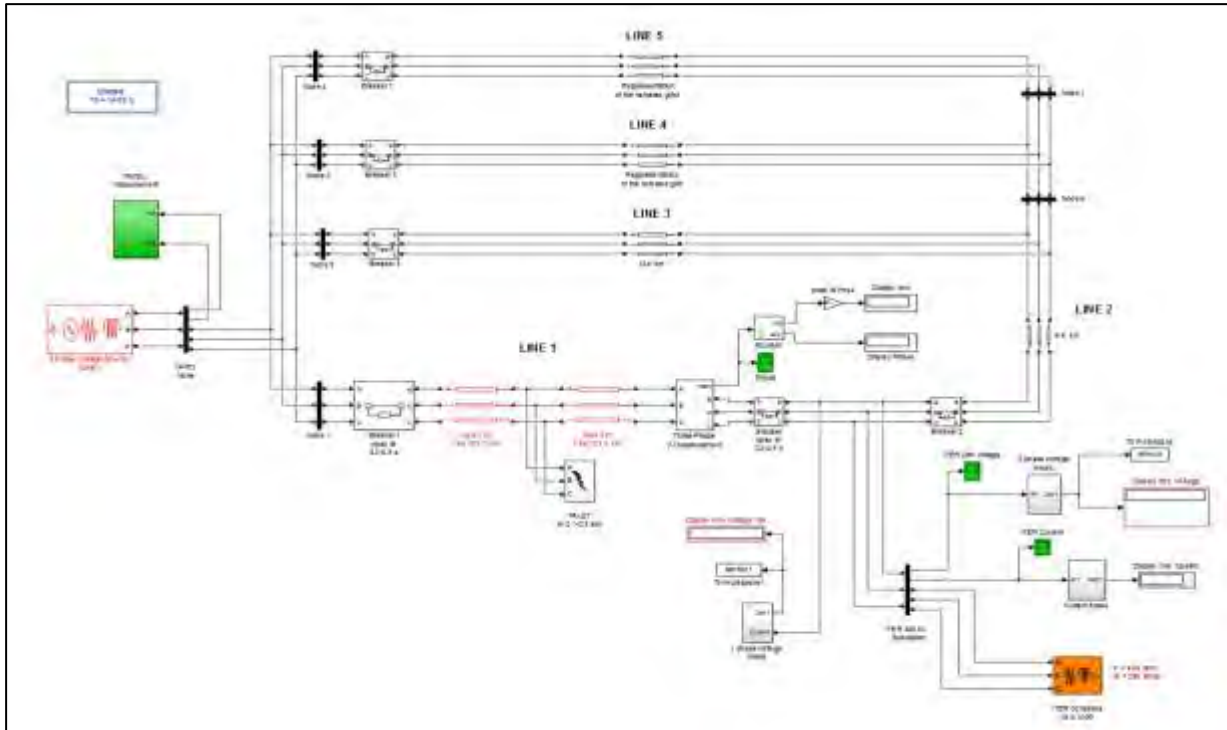


Fig. 5.3 Simulink model of the external grid

- The direct and zero sequence capacities are intended to respect the short circuit currents and based on realistic values:

	C_d [nF/km]	C_o [nF/km]
Line 1	0.134	8.57
Line 2	0.134	8.57

Tab. 5.5

With these values, together with the other ones reported in Tab. 5.1, the short circuit current in both the configurations is similar to that given by RTE;

- In Fig. 5.3 Line 1 is divided into two parts, with the total length equal to 125.7 km, in this way it is possible to apply the faults in different positions.

In addition, in the scheme there are several measurements blocks that are useful to control the values measured in various points and to understand if they are realistic or not.

The creation of this Simulink model has been difficult due to the need to represent of the remainder of the grid. First of all, there is no information regarding Boute Substations and its 220/400 kV transformers and so it cannot be directly reproduced in Simulink, but above all the entire electrical system is full of branches and other substations which provide ITER the required power and without knowing their characteristics and how they are distributed it is impossible to propose an accurate scheme.

Therefore the following has been created:

- The initial idea was that to insert in parallel to Line 1 and 2 one or more electrical lines and to adapt their impedances and lengths in order to obtain at ITER Prionnet the short circuit currents provided by RTE;
- The first values used for the resistance, inductance and capacity were similar to those of Line 1 and 2;
- Additional combinations have been tried, changing several times the number of the lines and then their characteristics, until reasonable results in term of the current were obtained. Finally, three other lines were added (Line 3, 4 and 5 in Fig. 5.3), because with just one the short circuit currents were correct only with a length of around 15-20 km, which is not realistic, but also because this is a better way to represent an extended electrical grid. Consequently, Line 3, 4 and 5 include Boutre Substation and also the rest of the system.

The values used in Tab. 5.6 are the results of the various attempts:

Equivalent Grid	R_d [Ohm/km]	R_o [Ohm/km]	L_d [mH/km]	L_o [mH/km]	C_d [nF/km]	C_o [nF/km]	d [km]
Line 3	0.0187	0.1603	0.56792	1.4515	0.2041	8.57	125
Line 4	0.0187	0.1603	0.86792	1.4515	0.1541	8.57	125
Line 5	0.0187	0.1603	0.86792	1.4515	0.1541	8.57	125

Tab. 5.6

With these data the short circuit currents and powers at Prionnet become the following:

ITER Prionnet	Maximum Configuration	Minimum Configuration
Isc L-L [kA]	15.67	5.82
Isc L-G [kA]	13.2	4.5
SC L-L Power [GVA]	11.942	4.032
SC L-G Power [GVA]	10.06	3.117

Tab. 5.7

The differences, as absolute values, between Tab. 5.2 and Tab. 5.7 are the following:

Differences	Maximum Configuration	Minimum Configuration
Isc L-L [kA]	0.23	0.22
Isc L-G [kA]	0.4	0
SC L-L Power [GVA]	0.175	0.152
SC L-G Power [GVA]	0.304	0

Tab. 5.8

It is evident that this Simulink model respects well enough the reality seen from ITER Prionnet, but nevertheless the biggest omission, and therefore the biggest error, of the scheme is the absence of other voltage sources: in fact in the simulations ITER receives power only from Tavel Substation, when in the reality it comes from several points and consequently this aspect compromises part of the results.

5.4 Simulations and Results

The simulations of the faults are applied only on Line 1 because compared with Line 2 it is longer (125.7 km) and so there is the possibility to see the impact even when this is applied beyond a distance of 9.6 km from ITER Prionnet, but also it is directly connected to the voltage source (Tavel Substation in the Simulink model); instead, in comparison with Line 3, 4 and 5, the data are reliable since they are provided by RTE.

At first the line-line and line-ground faults are performed directly at ITER Prionnet (distance equal to zero km) and then they are moved on Line 1 in direction of Tavel Substation with a step of 10 km at the time, until the end of the line.

The progression of the events is set in the following way:

- At the beginning, $t = 0$ seconds, the system is in steady state, with the voltage set at 400 kV in the three-phase source;
- At $t = 0.1$ seconds the fault is applied;
- At $t = 0.2$ seconds, so 100 milliseconds after the fault, the circuit breakers 1 and 2 (see Fig. 5.3) are open and remain in this state for 300 milliseconds;
- At $t = 0.3$ seconds the fault is solved and deleted;
- At $t = 0.5$ seconds the breakers are close, so 300 milliseconds after their opening.

During this succession the voltage is always kept at 400 kV at Tavel and it is not increase to 440 kV, because the aim of the analysis is to evaluate the voltage reduction and not the short circuit currents.

The results of the simulations are shown in the next tables and images.

a) Line-Line Fault:

Distance From Prionnet [km]	Voltage RMS [kV]	ΔV [%]
0	0.042	99.989
10	39.98	90.005
20	70.32	82.42
30	93.6	76.6
40	111.37	72.15

50	124.59	68.85
60	133.76	66.56
70	138.92	65.27
80	139.82	65.045
90	135.4	66.15
100	132.61	66.85
110	99.5	75.125
125.7	0.104	99.97

Tab. 5.9

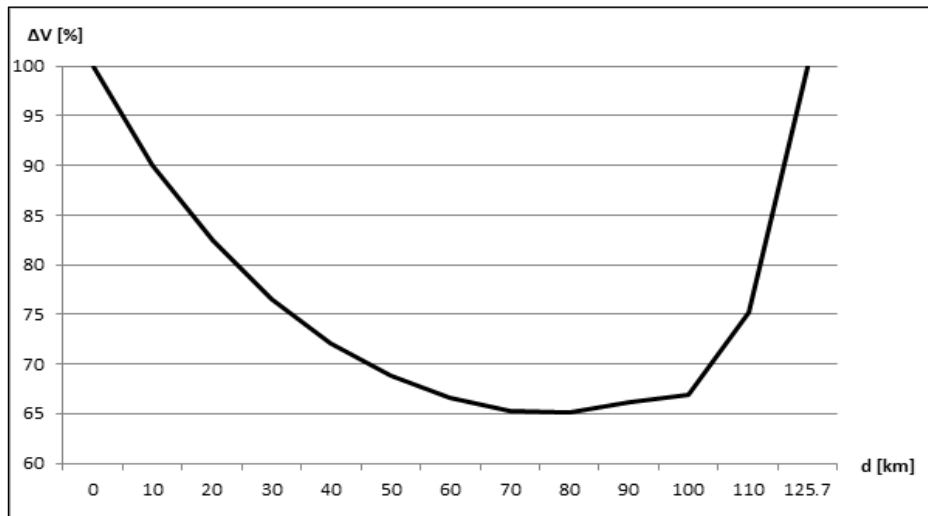


Fig. 5.4 Voltage Reduction with a line-line fault in different positions of Line 1

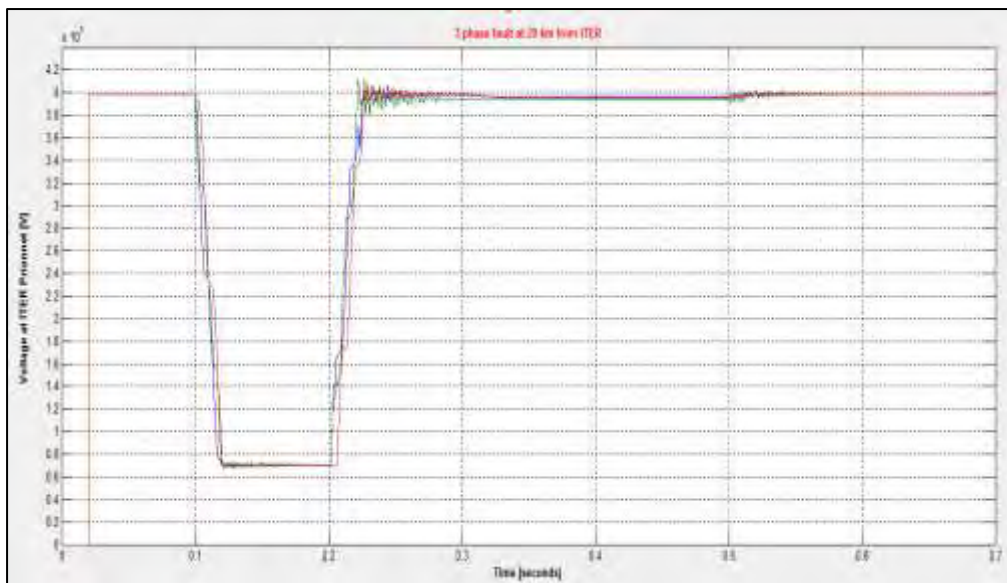


Fig. 5.5 Voltage profile with a three phase fault, $d = 20$ km

Note that $\Delta V\%$ is calculated in the following way:

$$\Delta V\% = \frac{V_r - V_{meas.}}{V_r} \cdot 100 \quad [5.4]$$

Where V_{meas} is the voltage measured and V_r is the rated voltage (in this case intended as phase-to-phase, so 400 kV).

What can be deduced from the previous table and images is that

- The highest voltage reduction is at ITER Prionnet ($d = 0$ km), as expected;
- Getting further from Prionnet the reduction is lower since ITER can receive power from the rest of the grid;
- Beyond a distance of 80 km the voltage starts to be reduced because the fault is closer to the only voltage source present in the model, so it is like that no other substation can provide ITER with power.

These results show that the analysis is acceptable up to a distance between 0 and 70 km, beyond this limit is unrealistic and therefore, when it is time to apply the reductions evaluated to the MV motors of busbars 43ALM1-JB-3000 and 4000, only the values included in the mentioned range are taken into account.

b) Line-to-ground Fault:

Note that the fault is always applied to phase 1.

Distance [km]	Phase 1 (Fault) [kV]	ΔV_1 [%]	Phase 2 [kV]	ΔV_2 [%]	Phase 3 [kV]	ΔV_3 [%]
0	0.14	99.94	238.5	-3.27	262.9	-13.84
10	27.96	87.89	236.67	-2.48	258.05	-11.74
20	48.55	78.98	235.4	-1.93	254.36	-10.14
30	64.05	72.26	234.45	-1.52	251.43	-8.87
40	75.8	67.17	233.72	-1.20	249.02	-7.83
50	84.59	63.37	233.11	-0.94	246.97	-6.94
60	90.86	60.65	232.58	-0.71	245.19	-6.17

Tab. 5.10

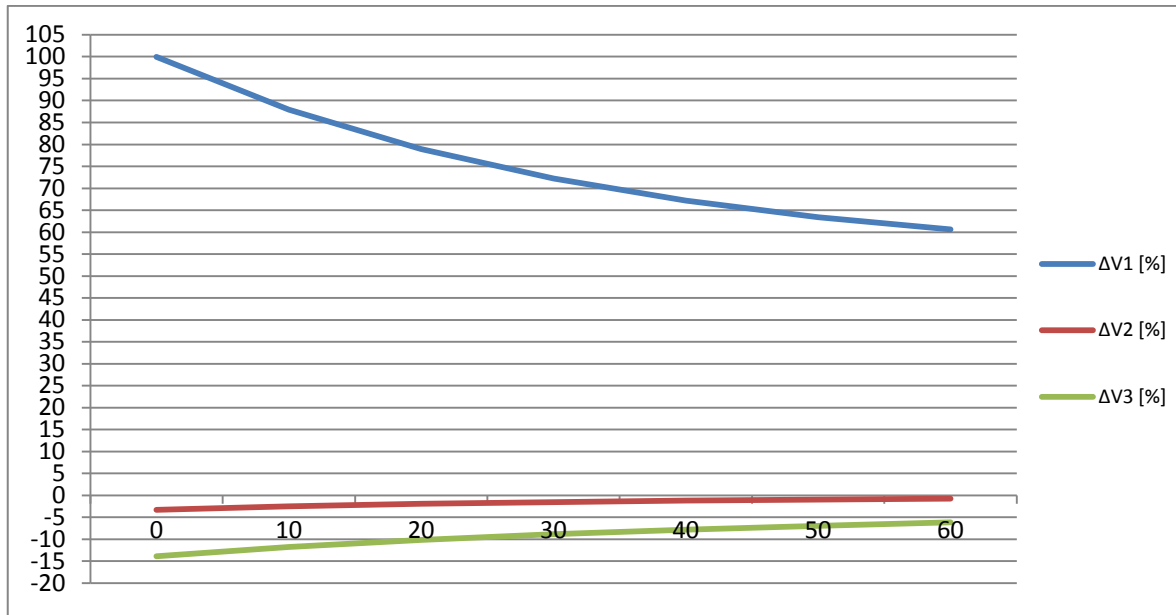


Fig. 5.6 Voltage Reduction with a line-ground fault in different positions of Line 1

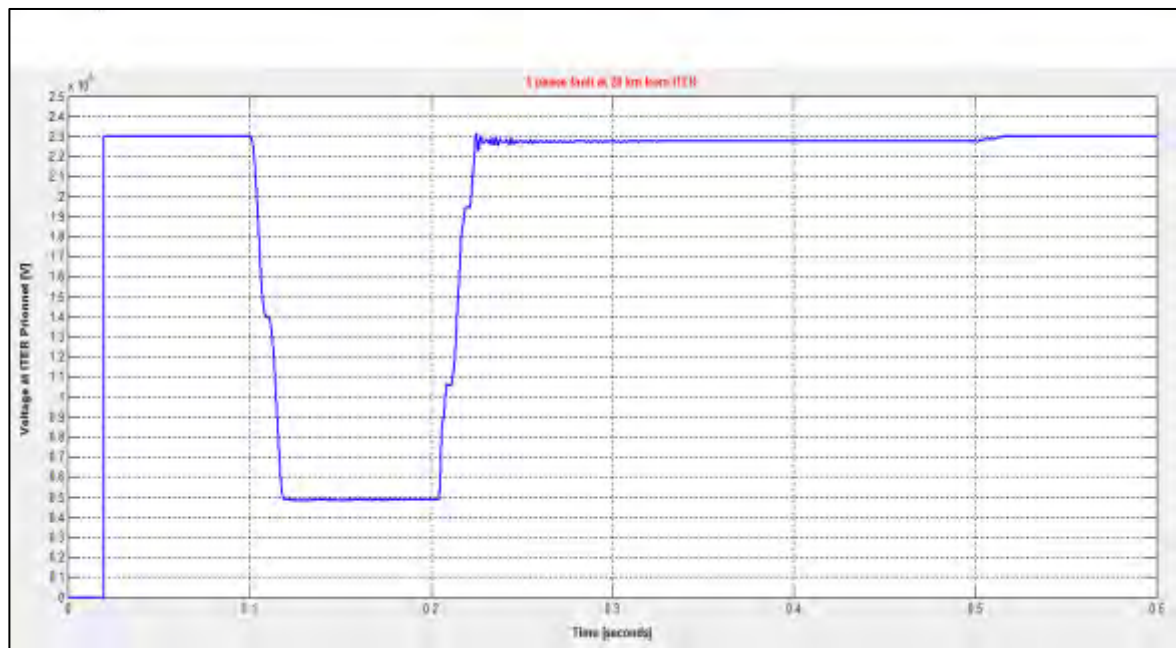


Fig. 5.7 Voltage profile with a line-ground fault, d = 20 km

In Tab 5.10 are shown the changes on all the phases and in fact

- Since the fault is applied on phase 1, this sees a reduction of the voltage magnitude, as foreseen;
- On the other side phase 2 and 3 are increased and this is why their ΔV is negative.

The line-line faults are not proposed for the results with distances greater than 60 km, because of the reason described previously regarding the inaccuracy of the Simulink model.

5.5 Effects on the MV Motors

The final goal of this analysis is to evaluate which impact could create such variations of voltage on the MV motors and their load and consequently understand if they could be dangerous for the fusion process.

To verify if the reductions of Tab. 5.9 and 5.10 could give problems to the system it is necessary to apply the calculated voltages on a Simulink model representing the ITER Network.

The model proposed in Fig. 5.8 is an extension of the one analysed in Paragraph 4.4 but with some difference:

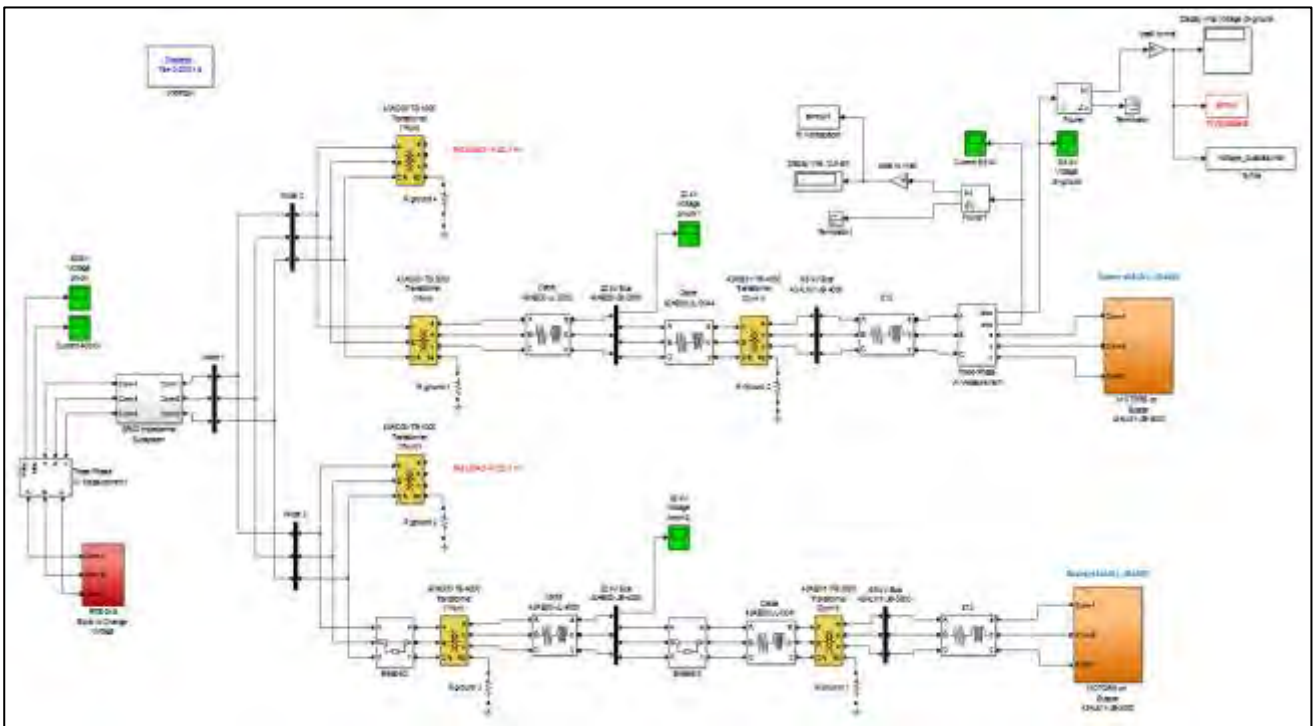


Fig. 5.8 ITER Network

- There are both busbars 43ALM1-JB-3000 and JB-4000, with all the MV motors shown in Fig. 3.1, and the four 400/22 kV transformers, because when a fault occurs on the external grid it is supposed that the entire plant will be in operation. Obviously, there is the possibility for the fault to happen in different scenarios. On the other side, with the starting analysis there was only a single branch with the LN2 GAN motor alone and not the entire ITER Network, because in the reality the various loads will be activated progressively and not simultaneously in order not to require much power at the same time from the electrical grid.
- The motors do not have to be started, they are already in a steady state condition at the beginning of the simulation: to do so in the motor block, in the *Initial Condition* entry field, there are the values of current (magnitude and phase) and the slip distinctive for the steady state. In this way it is not necessary to wait for the motors to complete the starting process and therefore the duration of the simulation is much shorter;

- The transformers 43AC00-TS-1000 and TS-3000 are not connected to any load, so their voltage is set at 23.1 kV, according to the datasheet. Their impedance is the same of the other two transformers (see Tab. 4.7);
- The biggest change is in the voltage source: in this instance the *Three Phase Voltage Source* block is not used because there is the necessity to manipulate the voltage in each single phase in order to apply the voltage calculated in Tab. 5.9 and 5.10. To do so the system shown in Fig. 5.9 has been created for all the three phases: note that in the image there is only the regulator of phase A, but in the model there is the same scheme for all the other two phases.

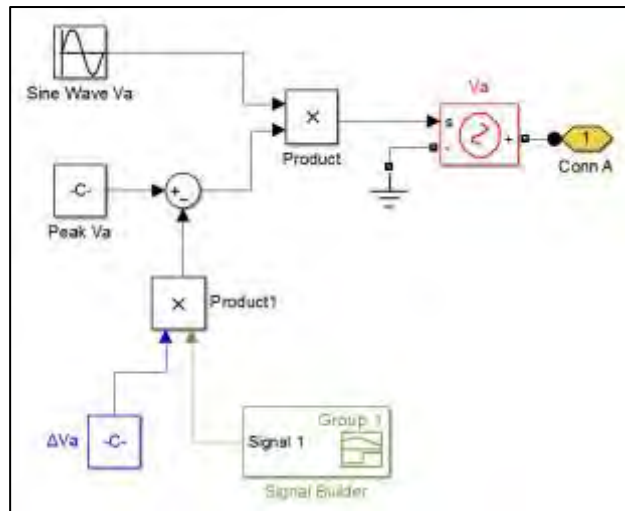


Fig. 5.9 Voltage Regulator – phase A

5.5.1 Voltage Source

This subsystem works in the following way:

- There are two constant blocks with the peak of the rated voltage in the Y configuration ($\sqrt{2/3} \cdot 400$ kV);
- The product between one of these blocks and a *Signal Builder* generates the reduction to be applied to the rated voltage: by managing the signal produced by this last block it is possible to modify the peak for a precise period. An example of this signal is shown in Fig. 5.10.

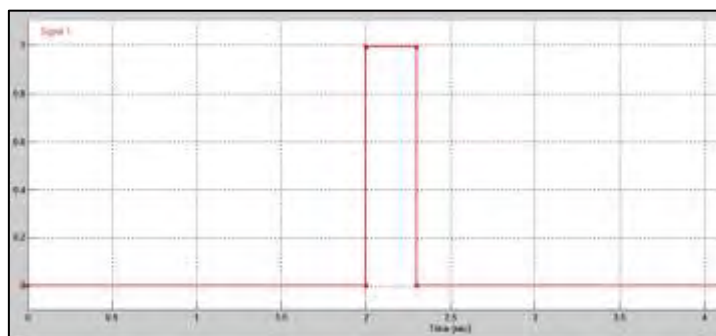


Fig. 5.10 Signal used to reduce the voltage

The vertical axis represents the ΔV wanted, the horizontal one the timeline.

- The result from the product is then added or subtract to the rated peak in order to increase or reduce it respectively: for example, a 100% reduction is reproduced by choosing $y = 1.00$ in the signal builder. For this study the ΔV is taken from Tab. 5.9 and 5.10, while the duration is set at 100 milliseconds;
- The final peak is eventually multiplied with a block that generates a sine wave with 1 as amplitude and a frequency of 50 Hz. It is important to respect the correct phase displacement between each of the three phases to avoid creating an unbalanced system; so the phases used are the ones reported in Tab. 5.11.

Phase	$\Delta\theta$ [°]
A	0
B	-120
C	-240

Tab. 5.11

5.5.2 Results

For the evaluation of the effects on both the electrical and mechanical side, the following procedure was implemented:

- To start, the reductions calculated for the faults at ITER Prionnet ($d = 0$ km) have been applied, because they are the greatest ones and so they could bring the worst impact on the Plant. To keep reproducing the worst scenario, both the busbars and their motors are connected and in operation;
- After having compared the minimum speed (n) reached by each MV motor during the process with the rated one, some calculation has been drawn and highlighted. If the speed is not in the admitted limits, it means that the reduction (and so the related fault) could be dangerous for the system and some consideration has to be made in order to avoid to stop the plant;
- If the results with the faults applied at Prionnet show that the speed limits are respected, then no other simulation has to be performed since the remaining reductions are not as big as the ones already applied to the Network. Vice versa, if the speed is over the limits other reductions will be analysed.

The speed limits to respect, shown in Tab. 5.12, are obtained from the torque-speed curves of the motors: the speed which gives the breakdown torque is the limit, because this forces the motor to be stopped. Consider also that with the breakdown torque there is a higher current to manage and this could force the circuit breakers to open, so putting the motor out of service.

It is important to note that it has not been established for what period this speed limit could be applied.

Speed Limit	4700 kW	2500 kW	1175 kW	986 kW
Speed [rpm]	2930	2936	2934	2820

Tab. 5.12

a) Line-line Fault at ITER Prionnet:

Distance [km]	ΔV [%]	Time [ms]
0	99.989	100

Tab. 5.13

This combination of voltage and time affects the speed as follows:

	4700 kW	2500 kW	1175 kW	986 kW
Minimum n [rpm]	2876	2720	2600	2650
Δn [%]	3.4	8.75	12.51	10.98
Total Duration [s]	0.6	0.6	0.6	0.6

Tab. 5.14

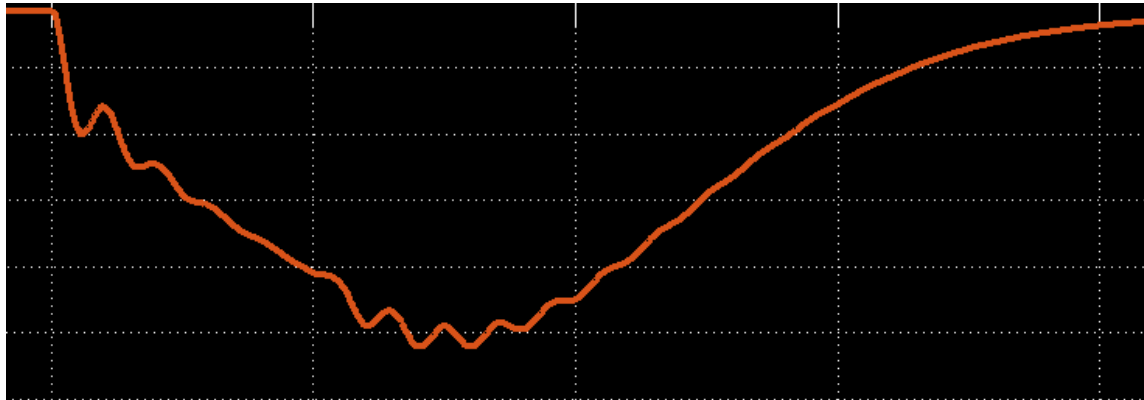


Fig. 5.11 Example of how the speed changes after the voltage reduction

As it can be seen from Tab. 5.14, the biggest change of speed happens in the 986 kW and 1175 kW motors because their inertia is much lower than the 4700 kW and 2500 kW motors: in fact, a big inertia is harder to decelerate and stop in a short period and this means that the LN2 GAN motor is less affected by this type of events. Comparing the results of Tab. 5.14 with the limits mentioned, what emerges is the following:

- Each motor goes beyond the limit;
- The minimum speed is reached for an instant and it does not last longer;
- The total variation (Δn) is about 600 milliseconds.

Due to the lack of precise information about the combination of the speed limits and their acceptable duration no definitive response can be proposed, but it can be said that

- The voltage reduction caused by a line-line fault at ITER Prionnet could affect the motors and their loads;
- There could be problems with the increased current and so with the opening of the circuit breakers;
- The analysis has to be updated and consequently a final judgement could be given only when there will be more details regarding these aspects of the motors.

In the following table it is summarized the replies of the motors to other reductions applied at a different distance from Prionnet, specifying if the speed limit is respected or not:

Distance [km]	4700 kW	2500 kW	1175 kW	986 kW
10	OK	NO	NO	OK
20	OK	NO	NO	OK
30	OK	NO	NO	OK
60	OK	NO	NO	OK

Tab 5.15

It can be noticed that

- The voltage reduction does not generate any speed concern to 4700 kW and 986 kW motors when the line-line fault strikes after 10 km;
- 2500 kW and 1175 kW motors still are affected even with the fault at 60 km. For the 2500 kW the speed is very close to the accepted limit, for the 1175 kW it is not the same (around 30 rpm beyond the limit)
- If the 1175 kW is connected to a VFD, which internally has a transformer, so the reaction during these transients could be different and the motor speed could be inside the admitted range.

b) Line-ground Fault at ITER Prionnet:

Distance [km]	ΔV_1 [%]	ΔV_2 [%]	ΔV_3 [%]	Time [ms]
0	99.94	-3.27	-13.84	100

Tab. 5.16

	4700 kW	2500 kW	1175 kW	986 kW
Minimum n [rpm]	2955	2955	2940	2946
Total Duration [s]	0.5	0.5	0.5	0.5

Tab. 5.17

A line-ground fault directly applied at ITER Prionnet does not seem to affect seriously the speed of the MV motors as was conversely seen with the line-line fault, because even if one phase has a magnitude equal to zero the other two can still create the phase-phase voltage and give power to the motors. Moreover the fault is very short and again the inertia plays a big part in limiting the reduction of speed.

In this case the speed limits are always respected: this means that a line-ground fault should not bring particular problems to these motors.

In conclusion, as shown and often underlined, this analysis has omissions that obviously bring errors and imperfections to the results: what is important to remember is the necessity to improve and update the models when more precise details are available.

6. Conclusions and Future Developments

This thesis is prevalently based on work to identify various dynamic related to the asynchronous motors connected to busbars MV-01, related to the Cryogenic system.

In the first part, chapters 2 and 3, are given some important detail on the motors and on how to use them inside ETAP and SimPowerSys: these evaluations represent a big and fundamental part of the work done at ITER, because the motor data can be changed often and it was the first time that this type of studies have been made.

Using the developed knowledge on ETAP and SimPowerSys and the theories of the power distribution, in the second part (chapter 4) it was analyzed the starting process of the LN2 GAN motor: in both softwares were found and used the most suitable settings, considering the study cases to perform and the options available. From the simulations came out that the 4.7 MW motor can have a huge impact on the ITER Electrical Network and on the external grid if it is started connected directly on line; so, coupling it with a soft starter set as shown, the effects on the voltage are considerably reduced and the limits imposed are always respected. The results from ETAP can be considered reliable since the comparison made with Simulink has proved that it represents well enough the electrical system examined. What can be done subsequently is to extend the SimPowerSys equivalent model in order to do other similar analyses for different portions of the SSEN.

In the last part, chapter 5, the impact on the MV motors caused by a fault on the external electrical grid was studied. This analysis is a sort of draft, because many details necessary to recreate the grid are not available and so many assumptions have been taken. The results obtained give an idea of how the MV-01 motors react to the faults and this can be considered as a starting point for this type of studies, because when more information regarding the grid and the SSEN will be provided it will be sufficient to update the current model built up in Simulink. Initially there was the idea to do the same simulations both in SimPowerSys and ETAP, but the latter is actually not complete for these study cases and therefore the comparison between the two softwares can be done when there will be upgrades in ETAP.

The most important aspect to keep in mind is that ITER is a project in continuous development which sees many changes, not only in the data to be used but in the analyses too, so everything reported in this thesis could be partially updated and modified or even totally changed in the future according to need of the project: for example, the number of MV motors, or their power, or the soft started connected could be different, so bringing the need of new analyses on the same topics done previously. What is also important is that the knowledge developed and shown in this thesis can be apply to other important electrical users inside the ITER network, such as the loads operating for the Cooling Water System and the Tritium Breeding System.

7. References

Note: The following documents with alphanumeric code are uniquely identified in ITER.

[1] **O. Motojima** - ITER DG - ITER: New technology for a New Industry - Enter Fusion technology Today between Research and production - Lesson Lecture - PISA University MScNE - May 10th 2013

[2] **R. Haange** - The ITER Project - Visit of Turkish Delegation in ITER Office - Saint Paul Les Durance September 2nd, 2013

[3] **Sergio Orlandi** - ITER Project: Lesson for a nuclear engineer - Enter Fusion Technology in ITER after thirty three years of experience in an industrial system on fission technology in Chernobyl and Fukushima - Lesson Lecture - PISA University MScNE - May 10th 2013

[4] **R. Haange** - ITER Project - Specific Goals, Progress and present status of Construction – Visit of EdF to ITER Office - Saint Paul Les Durance - September 2013

[5] **Sergio Orlandi** - Industrial policy and ITER Organization - An important challenge to assure industrial business opportunities - ITER Business Forum - Toulon France - March 21-22, 2013

[6] **G. Sanguinetti** - Preproduction Qualification for the ITER Divertor Inner Vertical Target – ITER Business Forum - Toulon France - March 21-22, 2013

[7] **M. Glugla** - Fuel Cycle: Design, Technologies and Schedule - ITER Business Forum Toulon France – March 21-22 2013

[8] **L. Serio** - Cooling Systems for ITER: Required Technologies, Design and Procurement status -ITER Business Forum - Toulon France - March 21-22 2013

[9] **I. Benfatto** - The ITER power supply systems and cable engineering - ITER Business Forum Toulon France – March 21-22 2013

[10] **Sergio Orlandi** - ITER Plant maintenance strategy and remote maintenance: Requirements for solutions - Together let us find cost effective solutions- TOBO Business Europe – Genova – April 11- 12 2013

[11] **Preliminary Safety Report for ITER - RPrS - 3ZR2NC - 12 Dec 2011 / 3.0 / Approved - Chapter 6.4.4: Power supply description - Pages 1/34**

[12] J.C. Gascon, J. Hourtoule, I. Benfatto, S. Nair, J. Tao, J. Goff - Design, Challenges and key Features for the ITER Electrical Power Distribution - ITER Organization, CS 90 046, 13067 St Paul Lez Durance, France

[13] Jeremy Goff1, José Gascon, Ashok Mankani, Inho Song - The ITER Magnet Power Supplies and Control System - ITER Organization, CS 90 046, 13067 St Paul Lez Durance, France

[14] European Iter Site Studies - EISS Cadarache - Report on the Functional Description of the ITER Plant for “Dossier d’Options de Surete” -GAC2-DEL-2001-00081 - June 2001

[15] J.C. Gascon - Design, challenges and key features for the ITER electrical power distribution - 15th International Conference on Emerging Nuclear Energy System - May 15-19, 2011 - Hyatt Hotel at Fisherman's Wharf San Francisco, California

[16] C. Neumeyer¹, I. Benfatto², J. Hourtoule², J. Tao², A. Mankani², F. Milani², S. Nair², I. Suh², H. Tan², M. Wang³, J.S. Oh⁴, A. Roshal⁵ - ITER Power Supply Innovations and Advances - ¹Princeton Plasma Physics Laboratory (PPPL), Princeton, NJ 08543-0451, USA, ²ITER Organization, Route de Vinon sur Verdon, 13115 Saint Paul-lez-Durance, France, ³China Int’l Nuclear Fusion Energy Program Execution Center (CN DA), 15B, FuXing Road, Beijing 100862, China, ⁴National Fusion Research Institute (NFRI), 169-148 Gwahak-ro, Yuseong-gu, Daejeon 305-806, Korea, ⁵ Federal State Unitary Interprise Efremov Scientific Research Institute of Electrophysical Apparatus (NIIEFA Efremov), 3, Road to Metallostroy, Metallostroy, St Petersburg, 196641, Russia

[17] ITER Design Report - System Functional Description - EPS (Emergency Power Supply) System 3F8KAD – 20th Sep 2012 - 1.3

[18] ITER - PPEN Power Loads Excel File - 2DXJJF - Power rating of PPEN Loads - Rev 2.4 - February 21st 2013

[19] L. Serio - Cryogenic System Introduction - ITER Business Forum – 1st October 2010

[20] V. Kalinin, E Tada, F. Millet, N. Shatil - ITER Cryogenic System – 27th Feb 2006

[21] ETAP 7.0.0 DEMO – Getting Started

[22] <http://en.wikipedia.org/wiki/MATLAB>

[23] Jörg Randermann – Starting and control of three-phase asynchronous motors – EATON

[24] ETAP Enterprise Solution for Electrical Power Systems – Online Help

[25] David Balaguer, Davide Cordioli - Motor starting analysis of 6.6kV LN2 GAN compressors using Soft-Starter – ITER Organization

[25] <http://www.iter.org/newsline/219/1145>

[26] RTE - Cahier des charges du systeme de protections d'ITER Organization, au poste de Prionnet 400 kV

[27] RTE - Référentiel Technique de RTE